14.2 Numerical Simulations: Solutions

This Section details the solutions of the simulation exercises proposed in Sec. 14.1.

Understanding these simulations requires having the code manual at hand, ready to consult, Zgoubi Users' Guide [1] in the present case, or whatever other code the reader my be willing to use otherwise.

In order to reproduce these numerical simulations, the code executable is required. Zgoubi package can be downloaded from its repository in sourceforge:

https://sourceforge.net/p/zgoubi/code/HEAD/tree/trunk/

A README file therein explains how the source code compiles to generate the executable, zgoubi. Running an optical sequence (say, Booster_Twiss.dat) is then just a matter of executing such command as

[pathTo]/zgoubi -in Booster_Twiss.dat

and results are listed, *a minima*, in zgoubi.res file, by default.

All necessary optical sequences for the simulation exercises have been provided as part of the assignments in Sec. 14.1, however most of the simulation material further discussed and used here (input data files, gnuplot scripts, etc.) is also available in the sourceforge repository, at

https://sourceforge.net/p/zgoubi/code/HEAD/tree/trunk/exemples/uspasSpinClass_2021/

Brief additional introductory guidance to using the code can be found in the Appendix, page 372.

14.2.1 Polarized Helion in AGS Booster

14.2.1.1 AGS Booster Parameters

Tab. 14.2 has been completed, yielding Tab. 14.37. Some derivations are detailed hereafter.

With $M = 2808.39$ MeV, $|G| = 4.18415$, and $dE/dN = q\hat{V}\sin(\phi_s) = 0.4$ MeV/turn (q=2, $\hat{V} = 0.4$ MV, $\phi_s = 30$ deg), the crossing speed comes out to be

$$\frac{dG\gamma}{d\theta} = \frac{1}{2\pi}\frac{G}{M}\frac{dE}{dN} = -9.4848 \times 10^{-5}.$$

The following excerpt from the 'print' file generated by a MAD8 computation of the Booster optical functions is aimed at allowing a comparison with Zgoubi

Table 14.37 AGS Booster parameters, table completed

Injection β		0.0655
Injection energy, kin.	MeV/u	2.0146
Injection $G\gamma$		-4.19316
Injection $B\rho$	T m	0.30745
Extraction energy, kin.	GeV/u	1.413059
Extraction $G\gamma$		-10.5
Extraction $B\rho$	T m	10.780516
Lattice		
Length	m	201.78
Tunes, ν_x, ν_y		4.73, 4.82
Chromaticities, ξ_x, ξ_y		-4.8, -5.2
Momentum compaction α		0.043998
Transition γ		4.7674
RF system		
revolution frequency, f_{rev}	MHz	0.09738 to 1.36362
RF harmonic		4
RF frequency	MHz	0.38953 to 5.45449
Peak voltage	kV	400
Synchronous phase	deg	30
Spin		
crossing speed $dG\gamma/d\theta$		-9.4848×10^{-5}

Table 14.38 Beam parameters, a copy of Tab. 14.3, for a reference

normalized emittances, ε_x, ε_y ($\pi\mu$m)		2.5
longitudinal emittance	eV s	0.50
momentum spread		$\pm 3\ 10^{-4}$

outcomes in the next question:

```
-----------------------------------------------------------------------------------------------------------
  Linear lattice functions.    TWISS          line: ASUPL6                    range: #S/#E
 Delta(p)/p:    0.000000      symm: F        super:  1                                              page   20
-----------------------------------------------------------------------------------------------------------
     ELEMENT SEQUENCE      I              H O R I Z O N T A L           I            V E R T I C A L
 pos.  element occ.    dist I  betax alfax   mux    x(co) px(co) Dx    Dpx  I  betay alfay   muy   y(co) py(co) Dy    Dpy
 no.   name    no.     [m]  I   [m]   [1]    [2pi]   [mm]  [.001] [m]   [1]  I   [m]   [1]   [2pi]  [mm]  [.001] [m]   [1]
-----------------------------------------------------------------------------------------------------------
 end   LA8      6  201.780   5.485 0.982  4.730  0.0000 0.000  0.739-0.104   9.704 -1.546  4.820 0.0000 0.000 0.000 0.000
 end   ASUPL    6  201.780   5.485 0.982  4.730  0.0000 0.000  0.739-0.104   9.704 -1.546  4.820 0.0000 0.000 0.000 0.000
 end   ASUPL6   1  201.780   5.485 0.982  4.730  0.0000 0.000  0.739-0.104   9.704 -1.546  4.820 0.0000 0.000 0.000 0.000
-----------------------------------------------------------------------------------------------------------
 total length =    201.780000       Qx       =      4.730145      Qy        =        4.820140
 delta(s)     =      0.000000 mm    Qx'      =     -7.313316      Qy'       =       -2.883899
 alfa         =    0.439414E-01     betax(max) =   13.545393      betay(max) =      13.149980
 gamma(tr)    =      4.770492       Dx(max)  =      2.909356      Dy(max)   =        0.000000
                                    Dx(r.m.s.) =    1.757448      Dy(r.m.s.) =       0.000000
                                    xco(max) =      0.000000      yco(max)  =        0.000000
                                    xco(r.m.s.) =    0.000000      yco(r.m.s.) =     0.000000
-----------------------------------------------------------------------------------------------------------
```

14.2.1.2 Cell and Lattice Optics

Questions 14.1.1.2.1-14.1.1.2.3 - Running superA.inc, due to the MATRIX command at the downstream end of the optical sequence, produces the first order trans-

port matrix of the super cell, say T_{cell}, and the corresponding beam matrix, *i.e.* the periodic optical functions at cell ends (using the relation $T_{\text{cell}} = I \cos \mu + J \sin \mu$).

These two matrices are found at the bottom of the computation listing, zgoubi.res.

Checking against the data in MAD8 'print' output file (Sec. 14.2.1.1) shows a very good agreement.

Question 14.1.1.2.4 - Running superA.inc with a TWISS command instead, produces, on the one hand, the following lattice parameter computation outcomes (similar to MATRIX outcomes), found down zgoubi.res listing (an excerpt):

```
*****************************************************************************************************************************
  112  Keyword, label(s) :  TWISS                                                                                IPASS= 4

              ******************************************************
              ************** End  of  TWISS  procedure **************
     There  has  been         4  pass  through  the  optical  structure

 Reference, before change of frame (particle #  1  - D-1,Y,T,Z,s,time)  :
  0.00000000E+00  -7.65859598E-13   2.62290190E-12   0.00000000E+00   0.00000000E+00   3.36300081E+03   3.68572492E-01
         Frame for MATRIX calculation moved by :
         XC =     0.000 cm , YC =   -0.000 cm ,    A =  0.00000 deg  ( = 0.000000 rad )

 Reference, after change of frame (particle #  1  - D-1,Y,T,Z,s,time)  :
  0.00000000E+00   0.00000000E+00   0.00000000E+00   0.00000000E+00   0.00000000E+00   3.36300081E+03   3.68572492E-01
 Reference particle (#      1), path length :   3363.0008     cm relative momentum :    1.00000

              TRANSFER  MATRIX  ORDRE  1  (MKSA units)
     -0.716001      -5.32491        0.00000        0.00000        0.00000       0.716859
      0.348220       1.19307        0.00000        0.00000        0.00000      -0.238490
      0.00000        0.00000        1.78816       -9.15235        0.00000       0.00000
      0.00000        0.00000        0.330121      -1.13043        0.00000       0.00000
     -7.886126E-02   0.414707       0.00000        0.00000        1.00000       1.58173
      0.00000        0.00000        0.00000        0.00000        0.00000       1.00000
       DetY-1 =     -0.0000004260,    DetZ-1 =     -0.0000004317
       R12=0 at     4.463    m,        R34=0 at    -8.096    m
   First order symplectic conditions (expected values = 0) :
   -4.2604E-07   -4.3171E-07    0.000        0.000        0.000        0.000

            TWISS  parameters,  periodicity  of   1  is  assumed
                         - COUPLED -
   Beam  matrix  (beta/-alpha/-alpha/gamma) and  periodic  dispersion  (MKSA units)
      5.483186      -0.982907       0.000000       0.000000       0.000000      0.742996
     -0.982907       0.358570       0.000000       0.000000       0.000000     -0.104814
      0.000000       0.000000       9.691428       1.545246       0.000000     -0.000000
      0.000000       0.000000       1.545246       0.349565       0.000000      0.000000
      0.000000       0.000000       0.000000       0.000000       0.000000      0.000000
      0.000000       0.000000       0.000000       0.000000       0.000000      0.000000
                     Betatron  tunes  (Q1 Q2 modes)
            NU_Y =  0.78833338        NU_Z =  0.80333330
                         Momentum compaction :
                    dL/L / dp/p =  4.39982231E-02
                         Transition gamma  =  4.76740921E+00
                         Chromaticities :
            dNu_y / dp/p = -0.80312438            dNu_z / dp/p = -0.86404335
*****************************************************************************************************************************
```

The TWISS command causes in addition the transport of the periodic optical functions throughout the sequence, logged in zgoubi.TWISS.out. These optical functions are displayed in Fig. 14.5.

Note: to produce this set of outputs, the TWISS command performs 4 consecutive passes through the optical sequence, see Users' Guide for details.

14.2.1.3 Spin Optics

The rigidity specified in the provided input data files and used in the previous question (superA.inc, etc.) is 1 T m. However, proper spin motion requires proper $G\gamma$ value! Thus, the rigidity in this exercise has to be changed to the injection value, namely (Tab 14.37),
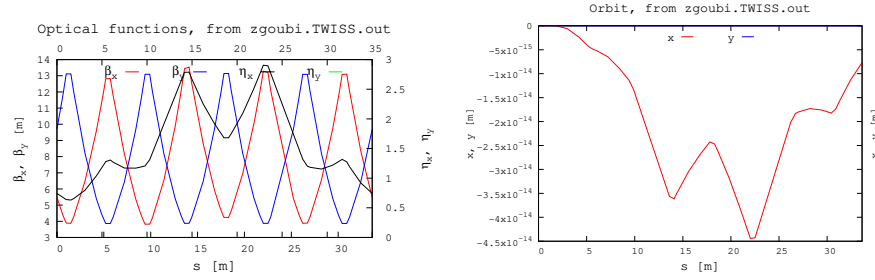
Fig. 14.5 Left: Booster super cell optical functions, from a TWISS computation. Right: it is not a bad idea to check what the horizontal and vertical orbits are, zero as expected in the present case

$$B\rho = 0.30745 \, \text{T m}$$

Question 14.1.1.3.1 - The spin motion of a helion is tracked along Booster for the case of an ideal ring (six superA cells, planar, no defects) using the input data file given in Tab. 14.7. One particle is taken on-momentum, the other two at $\delta p/p = \pm 10^{-4}$ and launched on their respective chromatic closed orbits, given the dispersion and its derivative (Sec. 14.2.1.2)

$$\eta_x = 0.743 \, \text{m}, \quad \eta'_x = -0.1048 \, \text{rad}$$

Tracking shows that the spin precession direction is vertical around the ring, for both on- and off-momentum particles (Fig. 14.6). This is what's expected as the

Fig. 14.6 Spins of 3 ions, respectively on- and $\pm 10^{-4}$ off-momentum, along their respective closed orbits around Booster. The vertical component S_Z is constant all along, thus the precession direction is vertical. S_X and S_Y are circling around the Z axis, in the bend plane
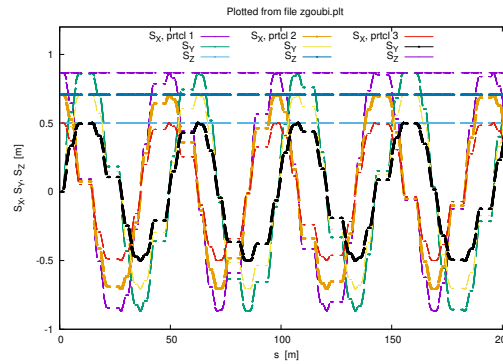
chromatic closed orbits also lie in the median plane: the field is everywhere vertical along a chromatic closed orbit as well, particles do not experience any horizontal field component, no field may kick spins away from vertical.

Questions 14.1.1.3.2, 14.1.1.3.3 - Tracking the spin closed orbit over a turn for particles at $dp/p = 0$ and $dp/p = \pm 10^{-4}$ off-momentum, yields spin motions displayed in Fig. 14.6.

Adding SPNPRT[MATRIX] allows for producing the spin matrices, however that also requires changing OBJET and SPNTRK data in Tab. 14.7, so to create 3 groups (as many as there are different momenta) of 3 particles each, as follows:

```
'OBJET'
0.3074552E3           ! Reference rigidity/kG.cm, for 3He++, at injection beta value 0.0655.
2             ! An option to define initial particle coordinates, one by one; here, 3 different
9 3       ! momenta, 9 particles; this is ordered to allow spin matrix computation by SPNPRT.
7.43281000E-03 -1.04862116E-02 0. 0. 0. 1.0001 'p'        ! Group 1. Orbit coordinates for a
7.43281000E-03 -1.04862116E-02 0. 0. 0. 1.0001 'p'             ! momentum offset of D=+1e-4.
7.43281000E-03 -1.04862116E-02 0. 0. 0. 1.0001 'p'
0. .0 0. 0. 0. 1. 'o'                          ! Group 2. On-momentum 3-particle set.
0. .0 0. 0. 0. 1. 'o'
0. .0 0. 0. 0. 1. 'o'
-7.42569731E-03 1.04862063E-02 0. 0. 0. .9999 'm'                       ! Group 3.
-7.42569731E-03 1.04862063E-02 0. 0. 0. .9999 'm'        ! Momentum offset of D=-1e-4.
-7.42569731E-03 1.04862063E-02 0. 0. 0. .9999 'm'
1 1 1 1 1 1 1 1 1

'PARTICUL'   ! Defining the particle species is necessary, in order for the program to solve
HELION                                             ! the T-BMT equation.
'SPNTRK'                              ! The 9 initial spins are organized so to allow spin matrix
4                        ! computation by SPNPRT, for each of the 3 different momenta concerned.
1. 0. 0.                                                       ! S_X, particle 1,
0. 1. 0.                                                       ! S_Y, particle 1,
0. 0. 1.                                                       ! S_Z, particle 1,
1. 0. 0.                                                       ! S_X/ particle 2,
0. 1. 0.                                                            ! etc.
0. 0. 1.
1. 0. 0.
0. 1. 0.
0. 0. 1.
```

This yields the following, including the spin transport matrix, fractional spin tune and precession axis, for each of the 3 momenta (an excerpt):

```
**********************************************************************************************************************
  641 Keyword, label(s) :  SPNPRT     MATRIX                                                              IPASS= 1

                      --  3  GROUPS  OF  MOMENTA  FOLLOW   --

                -----------------------------------------------------------------
                Momentum  group  #1 ; average  over 3 particles at this pass :
                      INITIAL                                  FINAL
      <SX>       <SY>       <SZ>       <|S|>           <SX>       <SY>      <SZ>       <|S|>    <G.gma>   <(SI,SF)>  sigma_(SI,SF)
                                                                                                          (deg)       (deg)
   0.333333   0.333333   0.333333   0.577350       -0.195770   0.428831   0.333333   0.577350  -4.193160  46.358429  32.780359

               Spin  components  of  each  of  the   3  particles,  and  rotation  angle :
                    INITIAL                                  FINAL
        SX        SY        SZ        |S|        SX        SY        SZ        |S|      GAMMA   |Si,Sf|  (Z,Sf_yz) (Z,Sf)
                                                                                               (deg.)   (deg.)   (deg.)
                                                                                           (Sf_yz : projection of Sf on YZ plane)
 p  1  1.000000  0.000000  0.000000  1.000000    0.349592  0.936902  0.000000  1.000000   1.0022   69.538   90.000   90.000    1
 p  1  0.000000  1.000000  0.000000  1.000000   -0.936902  0.349592  0.000000  1.000000   1.0022   69.538   90.000   90.000    2
 p  1  0.000000  0.000000  1.000000  1.000000    0.000000  0.000000  1.000000  1.000000   1.0022    0.000   45.000    0.000    3

               Min/Max  components  of  each  of  the   3  particles :
   SX_mi      SX_ma      SY_mi      SY_ma      SZ_mi      SZ_ma      |S|_mi     |S|_ma    p/p_0      GAMMA       I IEX
 3.4959E-01 3.4959E-01 9.3690E-01 9.3690E-01 0.0000E+00 0.0000E+00 1.0000E+00 1.0000E+00 1.00010E+00 1.00215E+00  1  1
-9.3690E-01 -9.3690E-01 3.4959E-01 3.4959E-01 0.0000E+00 0.0000E+00 1.0000E+00 1.0000E+00 1.00010E+00 1.00215E+00  2  1
 0.0000E+00 0.0000E+00 0.0000E+00 0.0000E+00 1.0000E+00 1.0000E+00 1.0000E+00 1.0000E+00 1.00010E+00 1.00215E+00  3  1

               Spin transfer matrix, momentum group # 1 :
            0.349592      -0.936902         0.00000
            0.936902       0.349592         0.00000
            0.00000        0.00000          1.00000
     Trace =      1.6991838357,  ;   spin precession acos((trace-1)/2) =      69.5376429739 deg
   Precession axis : ( 0.0000,  0.0000,  1.0000)  -> angle to (X,Y) plane,  angle to X axis :     90.0000,    90.0000 degree
   Spin  tune  Qs (fractional) :     1.9316E-01

                -----------------------------------------------------------------
                Momentum  group  #2 ; average  over 3 particles at this pass :
                      INITIAL                                  FINAL
      <SX>       <SY>       <SZ>       <|S|>           <SX>       <SY>      <SZ>       <|S|>    <G.gma>   <(SI,SF)>  sigma_(SI,SF)
                                                                                                          (deg)       (deg)
   0.333333   0.333333   0.333333   0.577350       -0.195765   0.428834   0.333333   0.577350  -4.193158  46.357996  32.780053

               Spin  components  of  each  of  the   3  particles,  and  rotation  angle :
```

```
                 INITIAL                                    FINAL
           SX        SY        SZ       |S|        SX        SY        SZ       |S|      GAMMA   |Si,Sf|  (Z,Sf_yz) (Z,Sf)
                                                                                                  (deg.)   (deg.)   (deg.)
                                                                                          (Sf_yz : projection of Sf on YZ plane)
 o  1  1.000000  0.000000  0.000000  1.000000    0.349603  0.936898  0.000000  1.000000   1.0022   69.537   90.000   90.000    4
 o  1  0.000000  1.000000  0.000000  1.000000   -0.936898  0.349603  0.000000  1.000000   1.0022   69.537   90.000   90.000    5
 o  1  0.000000  0.000000  1.000000  1.000000    0.000000  0.000000  1.000000  1.000000   1.0022    0.000   45.000    0.000    6

              Min/Max  components  of  each  of  the    3 particles :
  SX_mi      SX_ma      SY_mi      SY_ma      SZ_mi      SZ_ma      |S|_mi     |S|_ma       p/p_0       GAMMA          I  IEX
 3.4960E-01 3.4960E-01 9.3690E-01 9.3690E-01 0.0000E+00 0.0000E+00 1.0000E+00 1.0000E+00 1.00000E+00 1.00215E+00      4   1
-9.3690E-01 -9.3690E-01 3.4960E-01 3.4960E-01 0.0000E+00 0.0000E+00 1.0000E+00 1.0000E+00 1.00000E+00 1.00215E+00      5   1
 0.0000E+00 0.0000E+00 0.0000E+00 0.0000E+00 1.0000E+00 1.0000E+00 1.0000E+00 1.0000E+00 1.00000E+00 1.00215E+00      6   1

             Spin transfer matrix, momentum group # 2 :
        0.349603       -0.936898        0.00000
        0.936898        0.349603        0.00000
        0.00000         0.00000         1.00000
     Trace =      1.6992050586,    ;   spin precession acos((trace-1)/2) =      69.5369940370 deg
     Precession axis : ( 0.0000,  0.0000,  1.0000)  -> angle to (X,Y) plane, angle to X axis :    90.0000,    90.0000 degree
     Spin tune  Qs (fractional) :    1.9316E-01
             ---------------------------------------------------------
                   Momentum  group  #3 ; average  over 3 particles at this pass :
                 INITIAL                                    FINAL
      <SX>       <SY>       <SZ>      <|S|>        <SX>       <SY>       <SZ>      <|S|>     <G.gma>   <(SI,SF)> sigma_(SI,SF)
                                                                                                   (deg)        (deg)
 0.333333   0.333333   0.333333   0.577350     -0.195760   0.428836   0.333333   0.577350  -4.193157 46.357564 32.779748

              Spin  components  of  each  of  the     3 particles,  and  rotation  angle :
                 INITIAL                                    FINAL
           SX        SY        SZ       |S|        SX        SY        SZ       |S|      GAMMA   |Si,Sf|  (Z,Sf_yz) (Z,Sf)
                                                                                                  (deg.)   (deg.)   (deg.)
                                                                                          (Sf_yz : projection of Sf on YZ plane)
 m  1  1.000000  0.000000  0.000000  1.000000    0.349613  0.936894  0.000000  1.000000   1.0022   69.536   90.000   90.000    7
 m  1  0.000000  1.000000  0.000000  1.000000   -0.936894  0.349613  0.000000  1.000000   1.0022   69.536   90.000   90.000    8
 m  1  0.000000  0.000000  1.000000  1.000000    0.000000  0.000000  1.000000  1.000000   1.0022    0.000   45.000    0.000    9

              Min/Max  components  of  each  of  the    3 particles :
  SX_mi      SX_ma      SY_mi      SY_ma      SZ_mi      SZ_ma      |S|_mi     |S|_ma       p/p_0       GAMMA          I  IEX
 3.4961E-01 3.4961E-01 9.3689E-01 9.3689E-01 0.0000E+00 0.0000E+00 1.0000E+00 1.0000E+00 9.99900E-01 1.00215E+00      7   1
-9.3689E-01 -9.3689E-01 3.4961E-01 3.4961E-01 0.0000E+00 0.0000E+00 1.0000E+00 1.0000E+00 9.99900E-01 1.00215E+00      8   1
 0.0000E+00 0.0000E+00 0.0000E+00 0.0000E+00 1.0000E+00 1.0000E+00 1.0000E+00 1.0000E+00 9.99900E-01 1.00215E+00      9   1

             Spin transfer matrix, momentum group # 3 :
        0.349613       -0.936894        0.00000
        0.936894        0.349613        0.00000
        0.00000         0.00000         1.00000
     Trace =      1.6992262279,    ;   spin precession acos((trace-1)/2) =      69.5363467325 deg
     Precession axis : ( 0.0000,  0.0000,  1.0000)  -> angle to (X,Y) plane, angle to X axis :    90.0000,    90.0000 degree
     Spin tune  Qs (fractional) :    1.9316E-01
*********************************************************************************************************************
```

This simulation confirms the answer to Question 14.1.1.3.1.

The value of the spin precession angle is $\theta_{sp} = G\gamma\alpha$ modulo 360 degrees. The on-momentum value of $G\gamma\alpha$ can be found under PARTICUL in zgoubi.res (an excerpt):

```
*********************************************************************************************************************
     2  Keyword, label(s) : PARTICUL                                                                    IPASS= 1
     Particle  properties :
   HELION
             Mass          =    2808.39      MeV/c2
             Charge        =    3.204353E-19   C
             G  factor     =    -4.18415
             COM life-time =    1.000000E+99   s
         Reference  data :
             mag. rigidity (kG.cm)  :   307.45520     =p/q, such that dev.=B*L/rigidity
             mass (MeV/c2)          :   2808.3916
             momentum (MeV/c)       :   184.34550
             energy, total (MeV)    :   2814.4354
             energy, kinetic (MeV)  :   6.0438039
             beta = v/c             :   6.5499993689E-02
             gamma                  :   1.002152052
             beta*gamma             :   6.5640953062E-02
             G*gamma                :   -4.193158315
             electric rigidity (MeV) :  24.14925821   =T[eV]*(gamma+1)/gamma, such that dev.=E*L/rigidity
*********************************************************************************************************************
```

which yields a theoretical spin rotation of

$$|G\gamma| \times 360° = 4.193158315 \times 360° = 69.5369934 \, [360°]$$

(the on-momentum "group 2" above indicates 69.5369940370 deg) or equivalently a fractional spin tune value of

$$\nu_{sp} = 4.193158315/360 = 0.193158315$$

also in accord with the on-momentum "group 2" above which indicates 1.9316E-01.
  From theory (after Eq. 3.11, transposed to 3D space)

$$\text{frac}(\nu_{\text{sp}}) = \frac{1}{2\pi}\text{acos}\frac{\text{Trace(spin matrix)} - 1}{2}$$

whereas the spin matrix from tracking says (momentum "group 2" above)

$$\text{Trace}\,[\text{spin matrix}] = 1.6992050586$$

in accord with the previous spin tune value $\nu_{\text{sp}} = 0.193158$.

  Off-momentum (groups 1 and 3):

  γ needs to be corrected for the $dp/p = \pm 10^{-4}$ particles. The corresponding numerical results can be found under "group 1" and "group 3" above, respectively, and can be checked to agree with the theory.

14.2.1.4 Depolarizing Resonances

Question 14.1.1.4.1 - Locations ($G\gamma$ values) of the depolarizing resonances in the range

$$-10.5 \le \text{G}\gamma \le -4.19316$$

have been added to Tab. 14.8, yielding Tab. 14.39 (integer/imperfection resonances of the form $G\gamma = $ integer), and to Tab. 14.9, yielding Tab. 14.40 (systematic intrinsic resonances of the form $G\gamma = 6 \times$ integer $\pm Q_y$).

Question 14.1.1.4.2 - Figure 14.7 illustrates intrinsic resonance crossings with two graphs of $S_y(G\gamma)$, as follows:
    - a few particles are taken evenly distributed on the same vertical invariant ε_y; ε_x value does not matter, it is taken null here, as horizontal motion results in this perfect ring in only vertical perturbing field components - in quadrupoles - and these do not depolarize;
    - they are tracked from injection $G\gamma = -4.19316$ (Tab. 14.37) to $G\gamma = -16$, so crossing in particular the four strong resonances $G\gamma \pm \nu_y = 6n, \ |n| = 0 - 3$. Two different cases of the vertical invariant values are tracked: $\varepsilon_y = 2.5\,\pi\mu$m and 10 times less.

Table 14.39 Imperfection resonances, location and strengths. Strengths are normalized to the *rms* closed orbit value, $y_{co, rms}$ (the closed orbit is shown in Fig. 14.10). The "theory" column is filled-out using the thin lens model series

$G\gamma$ (Q. 14.1.1.4)	$|\epsilon_n|/y_{co, rms}$		
	theory (Q. 14.1.1.5)	tracking station.	crossing
-5	14.8696	13.8520	13.5490
-6	1.1779	1.0839	1.1917
-7	12.5802	11.5867	11.6697
-8	3.0465	2.9006	2.8585
-9	0.2637	0.2196	0.2373
-10	2.5296	2.7105	2.6408

Table 14.40 Systematic intrinsic resonances (M=6 super-periods, $\nu_y = 4.82$), location and strengths. The latter are normalized to $\sqrt{\varepsilon_y/\pi}$, with ε_y/π being the particle invariant value. The "theory" column is filled-out using the thin lens model series. The "station." (stationary) column is filled-out using $|\epsilon_n| \equiv \omega(\delta_n = 0)$, Question 14.1.1.6. Fill-out of the "crossing" column is addressed in Question 14.1.1.8 and Tab. 14.44

$kM \pm \nu_y$	$G\gamma$ (Q. 14.1.1.4)	$|\epsilon_n|/\sqrt{\varepsilon_y/\pi}$		
		theory (Q. 14.1.1.6)	tracking station.	crossing
$0 - \nu_y$	-4.82	3.3989	3.63	5.2
$-12 + \nu_y$	-7.18	3.1523	3.18	4.0
$-6 - \nu_y$	-10.82	7.9235	8.52	9.13
$-18 + \nu_y$	-13.18	11.072	11.8	12.5
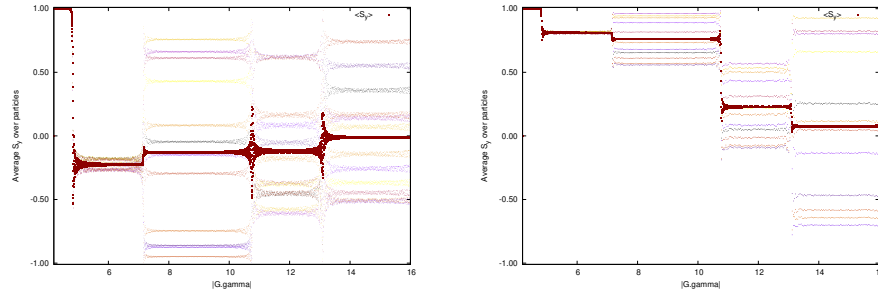
Fig. 14.7 Evolution of the vertical spin component of a few particles launched on the same invariant, with different initial betatron phases. The dark red curve is the average over 23 particles. Left: $\varepsilon_y = 2.5\,\pi\mu$m; right: $\varepsilon_y = 0.25\,\pi\mu$m.

Figure 14.7 is obtained with the following combined awk (left hand side) [11] and gnuplot (right) scripts:

```
! Average over particles of SZ values read in zgoubi.fai
function analyze(x, data){
    n = 0;mean = 0;      val_min = 0;val_max = 0;

    NBturns = 20000;
    Gg1 =4.193158; Gg2 =16; dGg = (Gg2-Gg1)/(NBturns-1);

    for(val in data){
        n += 1;
        delta = val - mean;
        mean += delta/n;
        val_min = (n == 1)?val:((val < val_min)?val:val_min);
        val_max = (n == 1)?val:((val > val_max)?val:val_max);
    }
    if(n > 0){
        print x, mean, val_min, val_max;
    }
}
{
    curr = $38*dGg + Gg1;     yval = $(col_num);

    if(NR==1 || prev != curr){
        analyze(prev, data);
        delete data;
        prev = curr;
    }
    data[yval] = 1;
}
END{
    analyze(curr, data);
}
```

```
set title "SZ(turn) and  <SZ(turn)>_particles"

nbtrj=100; evryNtrj = 5; evryNpass=9

NBturns = 20000
Gg1 =4.193158 ; Gg2 =16 ; dGg = (Gg2-Gg1)/(NBturns-1)

set xlab "turns"; set ylab "Average S_y over particles"
unset colorbox

fName = 'zgoubi.fai'
plotCmd(col_num)=sprintf('< gawk -f analyze.awk -v col_num=%d %s', col_num, fName)

set format y '%0.2f'
set xr [:20e3]; set xr [Gg1:Gg2]; set yr [-1.01:1.01]

plot for [it=1:nbtrj:evryNtrj] "zgoubi.fai" \
u ($26==it && evryNpass*int($38/evryNpass)==$38? $38*dGg + Gg1 :1/0):($22):($26) \
w p pt 7 ps .1 lc palette notit ,\
    plotCmd(22) u 1:2 w p pt 5 ps .4 lc rgb 'dark-red' t '<S_y>'
```
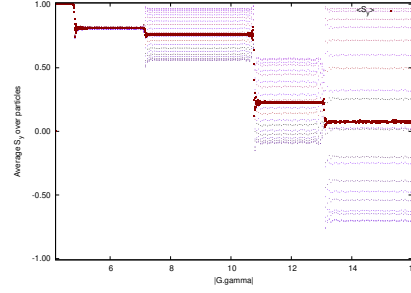
Fig. 14.8 A sensible question at this point is whether these results converge. The present figure is obtained using 200 particles. Comparison with the 23 trajectory case of Fig. 14.7 does not show much difference. The final polarizations is very similar, the problem converges

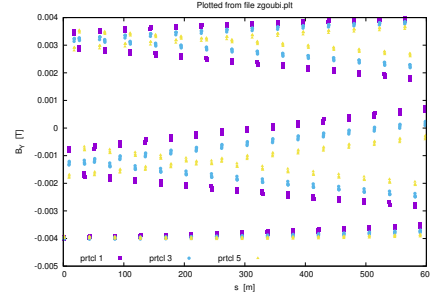- gnuplot script to obtain Fig. 14.9 from zgoubi.plt output file data:

```
set title "Plotted from file zgoubi.plt"
set key maxrow 1; set key b l

set xtics; set ytics

set xlabel 's  [m]'; set ylabel 'B_Y  [T]'

cm2m = 0.01 ; kG2T= 0.1
set xrange []
nbtrj = 5

plot for [i=1:nbtrj:2]   \
'zgoubi.plt' u ($19== i ? $14 *cm2m : 1/0): \
($24 *kG2T):($19) w p pt i+4 ps .9 lc i tit 'prtcl '.i
```


Fig. 14.9 Fields experienced in vertical quadrupoles during vertical betatron motion: 3 different particles are displayed here, over 3 turns around the ring. They are taken on the same invariant but with different initial betatron phases

When comparing these two graphs, essentially two things are observed: the spin kick across a resonance and the spin kick spread are smaller, when the invariant is smaller:

(i) a smaller invariant means smaller values of the perturbing $B_x = \mathcal{G}y$ radial field components in quadrupoles, hence smaller spin kicks;

(ii) spreading of betatron motion around the ring results from the spreading of the initial betatron phase of the particles for a given invariant. Smaller invariant value results in a smaller span of the field values experienced by the different particles in the vertical quadrupoles.

For the record: the resonance strength is $\propto \sqrt{\varepsilon_y/\pi}$ (Eq. 2.35).

Question 14.1.1.4.3 - A graph showing the span in magnetic field strengths experienced in the vertical quadrupoles by the 3 orbiting particles with the same invariant value, as an effect of their different initial betatron phases, is given in Fig. 14.9. The three vastly different torque series experienced by these particles' spins result in largely different spin states upon crossing the resonances (Fig. 14.7).

14.2.1.5 Imperfection Resonance Strengths

An excerpt of the input data file used is given in Tab. 14.41. It shows in particular

- sample vertical quadrupole misalignments accounted for by means of KPOS=5, which stick to Tab. 14.10 random vertical offset data;

- the use of FIT, preceding TWISS, which allows accounting for the non-zero vertical closed orbit excited by the quadrupole misalignments given in Tab. 14.10.

The vertical closed orbit so obtained in shown in Fig. 14.10.

The resonance strengths to be computed here, as a function of energy, all assume that very closed orbit (and obviously, the same optical functions).

Table 14.41 Head, intermediate quadrupoles, and tail of the Booster sequence, including vertical quadrupole misalignments, as well as a FIT-TWISS sequence which computes vertical orbit and optical functions (logged in zgoubi.TWISS.out), accounting for non-zero closed orbit (FIT first finds the orbit, prior to passing on to TWISS). The reference rigidity for this zgoubi.TWISS.out computation is arbitrary as the vertical orbit (and optical functions obviously) are maintained unchanged regardless of $G\gamma$ in these exercises (the fields are ramped to follow the value of the reference rigidity OBJET[BORO]). The final SYSTEM command causes execution of an external file, which plots the closed orbits and optical functions, reading the latter data from zgoubi.TWISS.out

```
Booster ring, complete, with vertical orbit.
'OBJET'
3.0428810404e+03
5
.001 .01 .001 .01 .001 .0001
0. 0. 0.84273180 1.5602297 0. 1. ' '
'PARTICUL'
HELION

'SCALING'
1 3
BEND
-1
3.04288104
1
MULTIPOL QH*   ! QH family is set for Qx=4.73 & Qy=4.82 tunes.
-1
3.30602909
1
MULTIPOL QV*   ! QV family is set for Qx=4.73 & Qy=4.82 tunes.
-1
3.24298881
1

'MARKER'    LA1S
'DRIFT'    DRIF    L057
57.0400
..............................................
'MULTIPOL' QVA1    QUAD
0  .Quad
0.493916E+02 10.0000 0.  -0.5472896982 0. 0. 0. 0. 0. 0. 0.
0. 0. 6.00  3.00 1.00 0.00 0.00 0.00 0.00 0. 0. 0.
6  .1122 6.2671 -1.4982 3.5882 -2.1209 1.723
0. 0. 6.00  3.00 1.00 0.00 0.00 0.00 0.00 0. 0. 0.
6  .1122 6.2671 -1.4982 3.5882 -2.1209 1.723
0. 0. 0. 0. 0. 0. 0. 0. 0. 0.
2.  ! cm  MultQVA1
5 0.0 0.0 0.67238500 0 0 0
..............................................
'MULTIPOL' QHA2    QUAD
0  .Quad
0.485016E+02 10.0000 0.   0.5256342158 0. 0. 0. 0. 0. 0. 0.
0. 0. 6.00  3.00 1.00 0.00 0.00 0.00 0.00 0. 0. 0.
6  .1122 6.2671 -1.4982 3.5882 -2.1209 1.723
0. 0. 6.00  3.00 1.00 0.00 0.00 0.00 0.00 0. 0. 0.
6  .1122 6.2671 -1.4982 3.5882 -2.1209 1.723
0. 0. 0. 0. 0. 0. 0. 0. 0. 0.
2.  ! cm  MultQHA2
5 0.0 0.0 0.73457500 0 0 0
..............................................
```

```
'MULTIPOL' QHF8     QUAD
0  .Quad
0.485016E+02 10. 0. 0.5256342158 0. 0. 0. 0. 0. 0. 0.
0. 0. 6.00  3.00 1.00 0.00 0.00 0.00 0.00 0. 0. 0.
6  .1122 6.2671 -1.4982 3.5882 -2.1209 1.723
0. 0. 6.00  3.00 1.00 0.00 0.00 0.00 0.00 0. 0. 0.
6  .1122 6.2671 -1.4982 3.5882 -2.1209 1.723
0. 0. 0. 0. 0. 0. 0. 0. 0. 0.
2.  ! cm  MultQHF8
5 0.0 0.0 0.38532700 0 0 0
'DRIFT'    DRIF    L031
29.9367
'BEND'    DHF8T    SBEN
0  .Bend
1.2096161E+02 0. 7.2121043E-01
0.00 0.00  0.00000000
4 .2401 1.8639 -.5572 .3904 0. 0. 0.
0.00 0.00  0.00000000
4 .2401 1.8639 -.5572 .3904 0. 0. 0.
1.0000E+00 cm  Bend
3 0. 0. 0.
'BEND'    DHF8Z    SBEN
0  .Bend
1.2096161E+02 0. 7.2121043E-01
0.00 0.00  0.00000000
4 .2401 1.8639 -.5572 .3904 0. 0. 0.
0.00 0.00  0.00000000
4 .2401 1.8639 -.5572 .3904 0. 0. 0.
1.0000E+00 cm  Bend
3 0. 0. 0.
'MARKER'    LA2E

'FIT'
2                                ! 2 variables, as follows.
1 32 0 [-1.,1.]          ! Allow +/-1cm variation of Z_0.
1 33 0 [-10.,10.]        ! Allow +/-10mrad variation of P_0.
2  1e-10     ! 2 constraints; requested penalty is 1e-10.
3.1 1 4 #End 0. 1. 0 ! Request final posit. Z=initial Z_0.
3.1 1 5 #End 0. 1. 0 ! Request final angle P=initial P_0.

'TWISS'
2 1. 1.
'FAISCEAU'     ! Allows quick check of initial=final Z, P.
'SYSTEM'       ! Plot closed orbits and optical functions.
1
gnuplot < ./gnuplot_TWISS.gnu
'END'
```

Resonance strength calculation uses (Eq. 2.29)
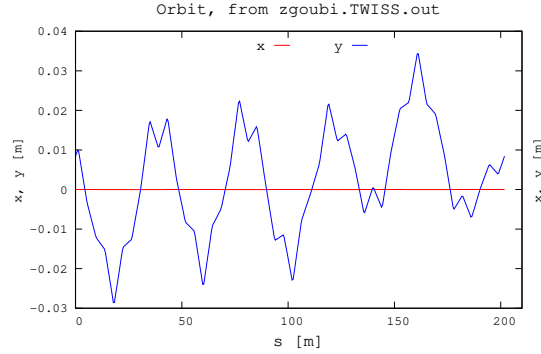
Fig. 14.10 Vertical closed orbit excited by the quadrupole misalignments of Tab. 14.10

$$\begin{Bmatrix} \mathcal{R}e(\epsilon_n^{\text{imp}}) \\ \mathcal{I}m(\epsilon_n^{\text{imp}}) \end{Bmatrix} = \frac{1 + G\gamma}{2\pi} \sum_{\text{Qpoles}} \begin{Bmatrix} \cos G\gamma\alpha_i \\ \sin G\gamma\alpha_i \end{Bmatrix} (KL)_i \ y_{co}(\theta_i)$$

which can be evaluated numerically. In this formula, the following data are read from zgoubi.TWISS.out at the locations of the quadrupoles (i index):

- θ_i: orbital angle, from the origin of the sequence,
- α_i: cumulative orbit deviation, from the origin of the sequence,
- $(KL)_i$: integrated quadrupole strength,
- $y_{\text{co},i}$: orbit excursion.

These quantities do not depend on $G\gamma$ (magnet fields are ramped to follow the value of the reference rigidity OBJET[BORO]).

Table 14.8 has been updated with the imperfection resonance strengths obtained this way yielding the "theory" column of Tab. 14.39.

14.2.1.6 Intrinsic Resonance Strengths

The optical functions and periodic vertical orbit are needed here, which means use of the output file zgoubi.TWISS.out. This file is produced using the input data file of the complete ring, equipped with a TWISS command, as in Sec. 14.2.1.2.

Resonance strength is obtained by summing the series (Eq. 2.35)

$$\begin{Bmatrix} \mathcal{R}e(\epsilon_n^{\text{intr}\pm}) \\ \mathcal{I}m(\epsilon_n^{\text{intr}\pm}) \end{Bmatrix} = \frac{1 + G\gamma}{4\pi} \sum_{\text{Qpoles}} \begin{Bmatrix} \cos(G\gamma\alpha_i \pm \varphi_i) \\ \sin(G\gamma\alpha_i \pm \varphi_i) \end{Bmatrix} (KL)_i \sqrt{\beta_{y,i} \frac{\varepsilon_y}{\pi}}$$

which can be calculated numerically. In this formula, the following data are read from zgoubi.TWISS.out at the locations of the quadrupoles (i index):

- θ_i: orbital angle, from the origin of the sequence,
- α_i: cumulative orbit deviation, from the origin of the sequence,
- $(KL)_i$: integrated quadrupole strength,
- φ_i: betatron phase advance,

- β_i: betatron function,
- ε_y/π: invariant value.

These quantities do not depend on $G\gamma$ (magnet fields are ramped to follow the value of the reference rigidity OBJET[BORO]).

For a reference, the upper and lower parts of zgoubi.TWISS.out data file (as produced by the TWISS command), showing the optical function values along the sequence needed to compute the series above are as follows (excerpts):

```
@ LENGTH         %le    33.63000810
@ ALFA           %le    0.5271462897E-01
@ ORBIT5         %le           -0
@ GAMMATR        %le    4.355463945
@ Q1             %le    0.7299999804      [fractional]
@ Q2             %le    0.8199999584      [fractional]
@ DQ1            %le   -0.7429052400
@ DQ2            %le   -0.8355856969
@ DXMAX          %le    3.01663095E+00    @ DXMIN          %le    9.49130311E-01
@ DYMAX          %le    0.00000000E+00    @ DYMIN          %le    0.00000000E+00
@ XCOMAX         %le    0.00000000E+00    @ XCOMIN         %le   -5.12842866E-14
@ YCOMAX         %le    0.00000000E+00    @ YCOMIN         %le    0.00000000E+00
@ BETXMAX        %le    1.41491375E+01    @ BETXMIN        %le    4.22123922E+00
@ BETYMAX        %le    1.27947203E+01    @ BETYMIN        %le    3.81920290E+00
@ XCORMS         %le    1.50372304E-14
@ YCORMS         %le    0.    not computed
@ DXRMS          %le    5.94727589E-01
@ DYRMS          %le    0.00000000E+00
@ DELTAP         %le    0.00000000E+00
@ |C|            %le    0.000000000
@ Q1*            %le    0.000000000
@ Q2*            %le    0.000000000
@ TITLE          %12s   "Zgoubi model"
@ ORIGIN         %12s   "twiss.f"
@ DATE           %08s   "   "
@ TIME           %08s   "   "
# From TWISS keyword
# alfx          btx           alfy          bty           alfl          btl           Dx            etc.
# 1             2             3             4             5             6             7
1.0086402E+000 5.8955920E+000 -1.5005233E+000 9.4500882E+000 0.0000000E+000 0.0000000E+000 1.1034842E+000 etc.
1.0086402E+000 5.8955920E+000 -1.5005233E+000 9.4500882E+000 0.0000000E+000 0.0000000E+000 1.1034842E+000
1.0086402E+000 5.8955920E+000 -1.5005233E+000 9.4500882E+000 0.0000000E+000 0.0000000E+000 1.1034842E+000
8.1346059E-001 4.8562657E+000 -1.6967856E+000 1.1273833E+001 0.0000000E+000 0.0000000E+000 1.0186499E+000
8.1346025E-001 4.8562641E+000 -1.6967859E+000 1.1273837E+001 0.0000000E+000 0.0000000E+000 1.0186498E+000
7.8964451E-001 4.7446880E+000 -1.7207337E+000 1.1511696E+001 0.0000000E+000 0.0000000E+000 1.0082983E+000

..........................................

1.6898235E+000 1.2487484E+001 -6.6866811E-001 4.1920085E+000 0.0000000E+000 0.0000000E+000 1.6554672E+000 etc.
1.3706530E+000 8.7748783E+000 -1.0863704E+000 6.3156052E+000 0.0000000E+000 0.0000000E+000 1.3317807E+000
1.0098358E+000 5.8871527E+000 -1.5040727E+000 9.4500414E+000 0.0000000E+000 0.0000000E+000 1.1034842E+000
1.0098358E+000 5.8871527E+000 -1.5040727E+000 9.4500414E+000 0.0000000E+000 0.0000000E+000 1.1034842E+000
1.0098358E+000 5.8871527E+000 -1.5040727E+000 9.4500414E+000 0.0000000E+000 0.0000000E+000 1.1034842E+000
1.0098358E+000 5.8871527E+000 -1.5040727E+000 9.4500414E+000 0.0000000E+000 0.0000000E+000 1.1034842E+000
```

A detailed description of zgoubi.TWISS.out data column format can be found in the Users' Guide, Section 8.4.

Table 14.9 has been updated with the intrinsic resonance strengths obtained here, yielding the "theory" column of Tab. 14.40.
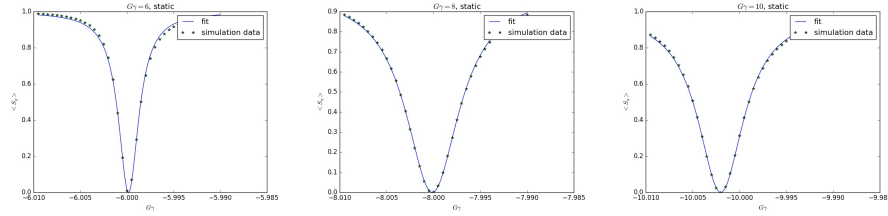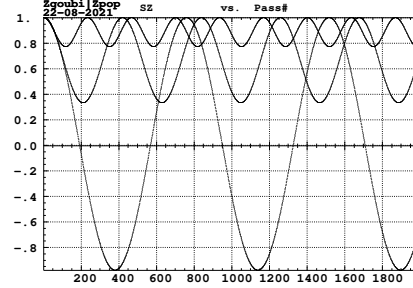
14.2.1.7 Spin Motion Through Imperfection Resonances

Input data files similar to those in the answer to Question 14.1.1.5 (Sec. 14.2.1.5 and Tab. 14.41) are used here. They only differ by

- the reference rigidity (OBJET[BORO]) and, accordingly, field coefficients under SCALING so to maintain unchanged orbit and optics,
- use of CAVITE for acceleration through the resonance, in the second question.

An interface has been developed in python (an evolution, by the present co-authors, of pyZgoubi [4]), which takes care of repeating the tracking at various distances $\Delta G\gamma = G\gamma - G\gamma_n$ from the resonance, in Question 14.1.1.8.1, or at various resonant frequencies $G\gamma_n$ in Question 14.1.1.8.2 thus automating the procedure.

Question 14.1.1.8.1 - The following shows the head and tail of the tracking input data file, in the stationary case, on the resonance $G\gamma_n = -6$. Note the INCLUDE of the SCALING segment [SCALING_S:SCALING_E] as defined in Tab. 14.7, with the field coefficient updated to present BORO/1000 value, namely, 4.8139470584

```
Booster
'OBJET'
4.8139470584e+03                                    ! Rigidity at G.gamma=-6.
2
1 1
0. 0. 0.84273180 1.5602297 0. 1. ' '        ! Track a single 3He, launched on closed orbit.
1
'PARTICUL'
HELION
'SPNTRK'                                            ! Start with spin vertical.
3
'FAISTORE'
zgoubi.fai
1

         ! Scaling coefficients in scaling_Gg6.inc are updated to present BORO/1000 value.
'INCLUDE'
1
scaling_Gg6.inc[SCALING_S,*:SCALING_E,*]

'DRIFT'    DRIF      L057
57.0400
..............
'BEND'     DHF8Z     SBEN
0  .Bend
1.2096161E+02   0.0000000E+00   7.2121043E-01
0.00  0.00   0.00000000
4 .2401  1.8639  -.5572  .3904 0. 0. 0.
0.00  0.00   0.00000000
4 .2401  1.8639  -.5572  .3904 0. 0. 0.
1.0000E+00 cm  Bend
3 0. 0. 0.
'MARKER'    LA2E                                    ! Booster lattice ends here.
'REBELOTE'  ! 2000 turns are sufficient to see a complete S_y oscillaiton when on resonance,
1999 0.1 99              ! from what <S_y> is deduced - greater distance to resonance
                                                    ! results in greater frequency.
'END'
```

Sample tracking results for $S_y(\theta)$ oscillation at various distances to the resonance, are given in Fig. 14.11. The average value $\langle S_y \rangle$ is computed from these tracking data.

The exercise is repeated for the different $-10 \leq G\gamma_n \leq -10$ values, resulting in Fig. 14.12 which shows $\langle S_y \rangle$ dependence on the distance to the resonance so obtained, and fit to Eq. 2.49

$$\langle S_y \rangle = \frac{\delta_n}{\sqrt{\epsilon_n^2 + \delta_n^2}} \qquad (14.5)$$

The "stationary" column of Table 14.8 has been completed accordingly (Tab. 14.39).

Question 14.1.1.8.2 - A 400 keV/turn acceleration rate is taken for the crossing ($\hat{V} = 400$ kV, synchronous phase 30 deg). The following shows the head and tail of the tracking input data file in the case of $G\gamma_n = -6$ crossing:

```
Booster
'OBJET'
3.77645661e+03                ! Initial rigidity is taken at Ggamma=-5.374744660,
2                             ! upstream enough not to feel the resonance at G.gamma=-6.
1 1
0. 0. 0.84273180 1.5602297 0. 1. ' '        ! Track a single 3He, launched on closed orbit.
1
'PARTICUL'
HELION
'SPNTRK'                                            ! Start with spin vertical.
```

Fig. 14.11 Spin oscilla-
tion $S_y(turn)$ for different
distances to the resonance
$G\gamma_n = -6$. A greater
distance δ_n results in a
higher oscillation frequency
$\omega = \sqrt{|\epsilon_n|^2 + \delta_n^2}$ (Sec. 3.5).
On the resonance, the preces-
sion axis lies in the median
plane, S_y oscillation covers
$[-1, 1]$ and $\langle S_y \rangle = 0$

Fig. 14.12 Average value of the vertical spin component S_y, depending on the distance to the
resonance for the cases of three different resonances $G\gamma_n = -6$, -8 and -10. The symbols are
from tracking, the solid curves are from the theory (Eq. 2.49). $\langle S_y \rangle = 0$ corresponds to S_y
oscillating over $[-1, 1]$, thus the precession axis lies in the median plane, $G\gamma$ is on resonance

```
3
'FAISTORE'
zgoubi.fai
1

            ! Scaling coefficients in scaling_GgXXX.inc are updated to present BORO/1000 value.
'INCLUDE'
1
scaling_Gg5.374.inc[SCALING_S,*:SCALING_E,*]

'MARKER'      LA1S                                        ! Booster lattice starts here.
'DRIFT'     DRIF      L057
57.0400
..............
'BEND'      DHF8Z      SBEN
0  .Bend
1.2096161E+02   0.0000000E+00   7.2121043E-01
0.00  0.00   0.00000000
4 .2401  1.8639  -.5572  .3904 0. 0. 0.
0.00  0.00   0.00000000
4 .2401  1.8639  -.5572  .3904 0. 0. 0.
1.0000E+00 cm  Bend
3 0. 0. 0.
'MARKER'      LA2E                                        ! Booster lattice ends here.
'CAVITE'
2
201.78 1.
4.e+05 0.5235987756                             ! 400 kV acceleration peak voltage.
'REBELOTE'      ! 2000 turns are sufficient to cross the resonance, leaving from away enough
1999 0.1 99                                     ! ending on the asymtotic region.
'END'
```

The initial $G\gamma$ is taken at -5.374744660, upstream enough not to feel the resonance
at $G\gamma_n = -6$.

Sample results for $S_y(\theta)$ during resonance crossing are given in Fig. 14.13, for
various $G\gamma_n = n$ values. The resonance strength are deduced from the respective
values of P_f/P_i, using (after Eq. 2.44)

$$|\epsilon_n| = \left(\frac{2\alpha}{\pi} \ln \frac{2}{1 + P_f/P_i} \right)^{1/2} \tag{14.6}$$

with $\alpha = \dfrac{dG\gamma}{d\theta} = 9.484 \times 10^{-5}$ being the resonance crossing speed.

This exercise is repeated for the different systematic resonances in $-10 \le G\gamma_n \le -10$, resulting in Fig. 14.12, which shows several cases of $\langle S_y \rangle$ dependence on the distances to the resonance so obtained, and fit to Eq. 2.49

$$\langle S_y \rangle = \frac{\delta_n}{\sqrt{\epsilon_n^2 + \delta_n^2}} \tag{14.7}$$
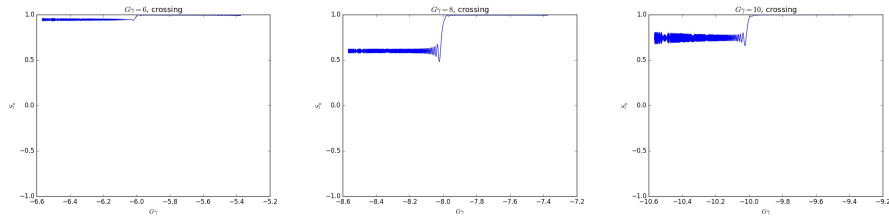
Fig. 14.13 Evolution of the vertical spin component S_y during integer resonance crossing, for the cases of $G\gamma = -6,\ -8$ and -10

The "crossing" column of Tab. 14.8 has been completed accordingly (Tab. 14.39).

14.2.1.8 Spin Motion Through Intrinsic Resonances

Questions 14.1.1.8.1, 2 - The systematic resonance at $G\gamma_n = 0 - \nu_y = -4.82$ is first considered, $B\rho = 2.67875735816\,\text{T\,m}$.

In the stationary case, the spin precession data are obtained by tracking a single particle with a particular vertical invariant value (use OBJET[KOBJ=8]) for many turns (use REBELOTE[NPASS=2000]) at a fixed energy.

The input data file is given in Tab. 14.42. It is similar to the input data file of Tab. 14.7, apart from the few necessary changes: modification the setup under OBJET (KOBJ=8 for a single particle with a certain invariant, on-momentum), SPNTRK, and addition of REBELOTE for multi-turn tracking. Note that the SCALING command and its data list, a segment defined in and included as a part of the input data file in Tab. 14.7, have been saved in the scaling_GgXXX.inc file, which is subject to an INCLUDE here. This is for the mere purpose of shortness. The values of the scaling coefficients in scaling_GgXXX.inc have to be updated to the present BORO value, for instance, in this case, from BORO/1000=0.3074552 (Tab. 14.7) to BORO/1000=2.678757358169758 (Tab. 14.42).

Table 14.42 Input data file for a 2000-turn tracking of spin motion, at fixed energy in the vicinity of the intrinsic resonance $G\gamma_n = 0 - \nu_y = -4.82$. Note that the SCALING command of Tab. 14.7 and its data list are subject to an INCLUDE (the scaling_GgXXX.inc file) for shortness

```
 'OBJET'
2.6787573581697584e3
    8
 1 1 1
 0. 0. 0. 0. 0. 1.
 0.982907  5.483186  0.
  -1.54525   9.69143  1.3196407949223E-07
 0. 1. 0.
 'PARTICUL'
  HELION
 'SPNTRK'
 4.1
 0. 0. 1.
 'FAISCEAU'
 'PICKUPS'
 1
 #Start
 'FAISTORE'
 zgoubi.fai
 1
  'MARKER'  #Start

        ! Scaling coefficients in scaling_GgXXX.inc are updated to present BORO/1000 value.
 'INCLUDE'
 1
 scaling_Gg4.82.inc[SCALING_S,*:SCALING_E,*]

 'INCLUDE'
 1
 6* superA.inc[superA_S,*:superA_E,*]

 'REBELOTE'
  2000 0.2 99

  'END'
```

The turn-by-turn spin motion obtained this way is displayed in Fig. 14.14. The slow oscillation in that graph is that of the vertical component S_y (S_Z in Zgoubi
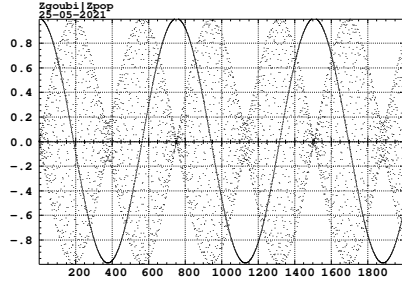
Fig. 14.14 Turn-by-turn motion of the three components of a spin, initially vertical. On-resonance here, $G\gamma = G\gamma_n = -\nu_y$, distance to the resonance $\delta_n = 0$. The slow oscillation (the solid curve with a 754 turn period) is that of the vertical component. The high frequency horizontal components (the high frequency dots, featuring the $\omega = |\epsilon_n|$ modulation) both average to zero, since s_π precesses about $\mathbf{n}$, which itself precesses about the vertical axis
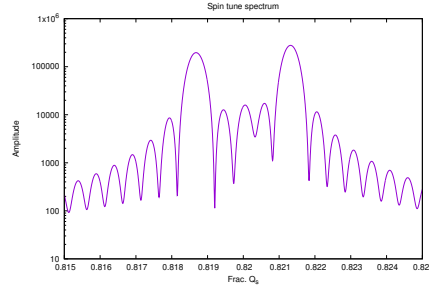
Fig. 14.15 Fourier spectrum of the spin motion (horizontal components). The two peaks at 0.82 ± 0.00135 are the result of combining the $G\gamma_n = 4.82$ frequency of $\mathbf{n}$ precession about the vertical axis and the $\sqrt{|\epsilon_n|^2 + \delta_n^2} = |\epsilon_n| = 0.00135$ frequency of the spin precession about $\mathbf{n}$

notation). The oscillation frequency is $\omega = \sqrt{|\epsilon_n|^2 + \delta_n^2} = |\epsilon_n|$. The amplitude averages to zero ($\langle S_y \rangle = 0$) in this case of being on resonance, since $\mathbf{n}$ is in the horizontal plane, namely (Eq. 2.48)

$$\delta_n = 0 \qquad \text{thus} \qquad |s_\pi|^2 = \frac{1}{1 + \left(\dfrac{\delta_n}{|\epsilon_n|}\right)^2} = 1 \quad \Rightarrow \quad \langle S_y \rangle = \sqrt{1 - |s_\pi|^2} = 0$$

The horizontal components S_x and S_s (S_Y and S_X in Zgoubi notations) are also displayed (fast oscillatory motion appearing as scattered dots). They oscillate at a much greater frequency $G\gamma_n \gg \omega$. They average to zero, since the eigenvector $\mathbf{n}$ precesses about the vertical axis with a constant projected n_y component independent of the turn number. Figure 14.15 shows the Fourier spectrum of the motion. On-resonance ($\delta_n = 0$), the oscillation frequency (in units of revolution frequency) is (see Sec. 3.5)

$$\omega \equiv \sqrt{|\epsilon_n|^2 + \delta_n^2} \overset{\delta_n=0}{=} |\epsilon_n| = 1/754 = 0.00133$$

Given that the period of the slow motion in Fig. 14.15 is about 754 turns, the value of 0.00133 is in a good accord with the distance of the peaks in Fig. 14.15 to frac($G\gamma_n$) = 0.82. Two additional distances to the resonance, $\delta_n = |\epsilon_n|$ and $\delta_n = 2|\epsilon_n|$, are displayed in Fig. 14.16.

Stationary tracking can be repeated for the other three systematic intrinsic resonances. The "stationary" column of Table 14.9 has been completed accordingly (Tab. 14.40).
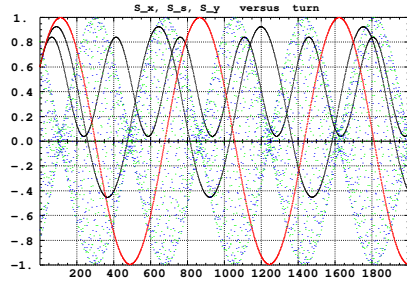
Fig. 14.16 Helion spin precession at $G\gamma = -\nu_y$ in the AGS Booster. S_y oscillates slowly (the solid sine waves), frequency $\omega \ll 1$. Three different distances to the resonance are plotted: $\delta_n = 0$ (the slow wave with a ± 1 amplitude), $\delta_n = |\epsilon_n|$ and $\delta_n = 2|\epsilon_n|$ (the fast wave with the smallest amplitude). S_x and S_s exhibit fast oscillations (dots) at a frequency $G\gamma_n = 4.82 \gg \omega$ modulated by the frequency ω

Questions 14.1.1.8.3, 4 - A 100 keV/turn acceleration rate is taken for crossing ($\hat{V} = 100$ kV, synchronous phase 30 deg). However, this is an arbitrary choice. The resonance strength does not depend on the crossing speed, so $\hat{V}$ is a free parameter.
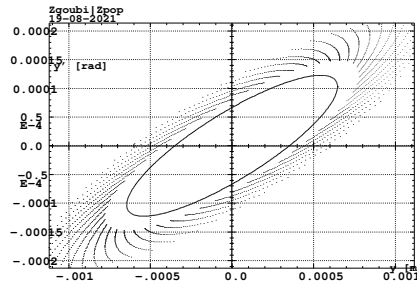
Fig. 14.17 Particle motion in the vertical phase space over the 2000-turn acceleration range (dots) in the case of $|G\gamma_n| = \nu_y$. The particle invariant is damped, from an initial $\varepsilon_{y,i}/\pi$ to a final $\varepsilon_{y,f}/\pi$ value. The solid ellipse is the *rms* ellipse matched to the 2000-turn damped motion
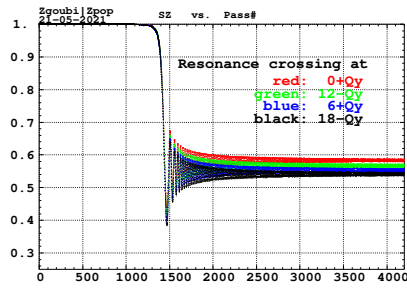
Fig. 14.18 Crossing of each of the four systematic resonances is displayed here. In each case, three particles are tracked. They are launched with $2\pi/3$ (normalized) betatron phase spacing. These three different curves essentially superimpose (they cannot be distinguished on this graph), *i.e.*, P_f is independent of the initial ϕ_y. The starting $G\gamma$ value is $100 \times |\epsilon_n|$ upstream of the resonance. The particle invariant is chosen to ensure $P_f/P_i \approx 0.5$.

The four systematic resonance cases, namely, $G\gamma_n = $ integer $\times M \pm \nu_y$ (M=6 cells), are tracked to fill out Tab. 14.40. The resonance strengths are deduced from the respective values of P_f/P_i, using (after Eq. 2.44)

$$|\epsilon_n| = \left(\frac{2\alpha}{\pi} \ln \frac{2}{1 + P_f/P_i} \right)^{1/2} \tag{14.8}$$

Table 14.43 Input data file for a 4504-turn helion ion acceleration across $G\gamma_n = 0 - \nu_y = -4.82$ at a rate of $100\,\text{keV/turn}$. Note that the value of the scaling coefficient in scaling_GgXXX.inc has to be updated to the present value of BORO/1000=2.12998742

```
4504-turn helion ion acceleration
 'OBJET'                                                                                    1
    2.12998742d3
    8
 1 3 1
0. 0. 0. 0. 0. 1.
0.982907  5.483186  0.
   -1.54525         9.69143        1.864270E-07
0. 1. 0.
 'PARTICUL'
  2.808391586E+03  3.204352974E-19  4.184153800E+00  0. 0.
 'SPNTRK'
 3
 'FAISCEAU'
 'PICKUPS'
 1
#Start
 'FAISTORE'
 b_zgoubi.fai  #End
 1
 'MARKER'  #Start

         ! Scaling coefficients in scaling_GgXXX.inc are updated to present BORO/1000 value.
 'INCLUDE'
 1
 scaling_Gg4.596.inc[SCALING_S,*:SCALING_E,*]

 'INCLUDE'
 1
 6* superA.inc[superA_S,*:superA_E,*]

 'CAVITE'
 3
   201.78004860000      1.00
  1.00000000E+05     5.235987755983E-01
 'MARKER'   #End
 'REBELOTE'
    4503  0.2  99

 'END'
```

Table 14.44 Asymptotic final polarization P_f, starting from $P_i = 1$. The particle invariant is damped over the 2000-turn acceleration range, from $\varepsilon_{y,i}/\pi$ to $\varepsilon_{y,f}/\pi$. $\langle \varepsilon_y/\pi \rangle$ is twice the final *rms* ε_y/π value (*i.e.*, the area enclosed by the *rms* ellipse matched to the damped motion in the phase space)

$|G\gamma_n|$	P_f	$\varepsilon_{y,i}$	$\varepsilon_{y,f}$	$\dfrac{|\epsilon_n|}{\sqrt{\langle \varepsilon_y/\pi \rangle}}$
		[μm]	[μm]	
$0 + \nu_y$	0.584	0.162	0.099	5.2
$12 - \nu_y$	0.565	0.25	0.218	4.1
$6 + \nu_y$	0.554	0.0476	0.0442	9.13
$18 - \nu_y$	0.545	0.0261	0.0246	12.5

with the resonance crossing speed of $\alpha = \dfrac{dG\gamma}{d\theta} = 2.371 \times 10^{-5}$.

The particle invariant is chosen to ensure $P_f/P_i \approx 0.5$, for convenience. For each $G\gamma_n$ value, three particles are tracked. They are launched with $2\pi/3$ (normalized) betatron phase spacing. It can be observed, however, (Fig. 14.18) that these four different spin motions $S_y(\text{turn})$ essentially superimpose (this would not be the case above a sufficiently large ε_y value causing substantially different betatron excursions

along the ring), which implies, in particular, that the asymptotic P_f is independent of the initial ϕ_y for a given invariant ε_y.

Particle motion in the vertical phase space is displayed in Fig. 14.17. The motion is damped due to acceleration. The spin motion is displayed in Fig. 14.18. The starting $G\gamma$ value is taken $100 \times |\epsilon_n|$ upstream of the resonance, so that the **n** vector is essentially vertical (for a reference: $7 \times |\epsilon_n|$ corresponds to $\cos\phi = \langle S_y \rangle = 0.99$).

The input data file for the case $G\gamma_n = 0 + \nu_y$ is given in Tab. 14.43. The same file is used for the other three resonances. The only changes are the updated values of BORO under OBJET and of the scaling coefficients in the INCLUDEd file scaling_GgXXX.inc (namely, the latter are updated to BORO/1000).

Table 14.44 summarizes the asymptotic P_f values obtained this way for the four systematic intrinsic resonances, and the resulting resonance strengths $|\epsilon_n|$ obtained using Eq. 14.6 with $P_i = 1$. The "crossing" column of Tab. 14.9 has been completed accordingly (Tab. 14.40).

14.2.1.9 Spin Motion Through a Weak Resonance

The systematic intrinsic resonance

$$G\gamma_n = -\nu_y = -4.8201$$

is considered, under fast crossing,

$$\hat{V} = 400\,\text{kV}$$

The tune value $\nu_y = -4.8201$ above results from the lattice settings (Sec. 14.2.1.2). Fourier analysis of the multiturn phase space motion displayed in Fig. 14.17 confirms that value.

Compared to the previous simulations, the four times greater acceleration rate here weakens the depolarizing effect. the resonance is made weaker in addition by using a smaller invariant, namely

$$\varepsilon_y/\pi \approx 1.03 \times 10^{-8}$$

at the resonance (the invariant damps during acceleration, the starting value is $\varepsilon_y/\pi \approx 1.3 \times 10^{-8}$ m, Tab. 14.45). The input data file for this tracking is given in Tab. 14.45, a copy of Tab. 14.43, *mutatis mutandis*, namely: with the initial invariant changed to $\varepsilon_y/\pi \approx 1.3 \times 10^{-8}$ under OBJET, the peak voltage changed to $\hat{V} = 400\,\text{kV}$ under CAVITE, and NPASS=2000 under REBELOTE. This results in

$$P_f \approx 0.9906\,P_i$$

as can been seen from Fig. 14.19 showing a graph of the turn-by-turn S_y(turn) motion across the resonance.

Fitting that spin motion S_y(turn) to the Fresnel integral model (Eq. 2.47)

Table 14.45 Input data file for 2001-turn helion ion acceleration across $G\gamma_n = -\nu_y = -4.82$ at a rate of 400 keV/turn. Note that the value of the scaling coefficient in scaling_GgXXX.inc has been updated to the present value of BORO/1000=2.12998742

```
Crossing a weak resonance
'OBJET'
   2.12998742d3
   8
1 3 1
0. 0. 0. 0. 0. 1.
0.982907 5.483186  0.
  -1.54525        9.69143        1.31964E-08
0. 1. 0.
'PARTICUL'
 2.808391586E+03  3.204352974E-19  4.184153800E+00  0. 0.
'SPNTRK'
3
'FAISCEAU'
'PICKUPS'
1
#Start
'FAISTORE'
zgoubi.fai  #End
1
'MARKER'  #Start

         ! Scaling coefficients in scaling_GgXXX.inc are updated to present BORO/1000 value.
'INCLUDE'
1
scaling_Gg4.596.inc[SCALING_S,*:SCALING_E,*]

'INCLUDE'
1
6* superA.inc[superA_S:superA_E]

 'CAVITE'
 3
   201.78004860000      4.00
   4.00000000E+05     5.235987755983E-01

'MARKER'   #End

'REBELOTE'
2000  0.2  99

'END'
```


Fig. 14.19 A graph of $S_y(\text{turn} = \theta/2\pi)$. The symbols show the tracking results. The solid curve represents the Fresnel integral model.
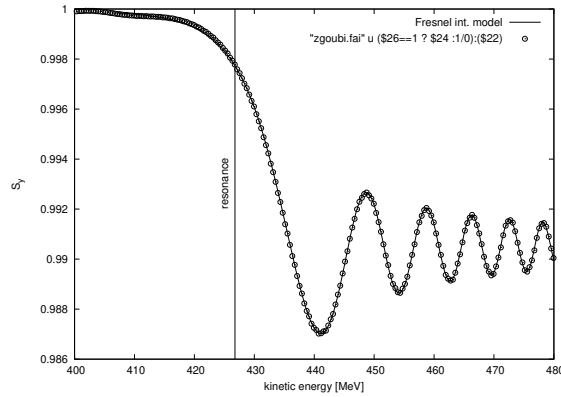
downstream of the resonance

For $y > 0$ *i.e.,* $\theta > 0$ $\quad \rightarrow \sin^2\varphi = \dfrac{\pi}{a}\,|\epsilon_n|^2\left[(0.5 + C(y))^2 + (0.5 + S(y))^2\right]$

For $y < 0$ *i.e.,* $\theta < 0$
pose $y = -x$ with $x > 0$ $\quad \rightarrow \sin^2\varphi = \dfrac{\pi}{a}\,|\epsilon_n|^2\left[(0.5 - C(x))^2 + (0.5 - S(x))^2\right]$

upstream of the resonance

yields the respective resonant $G\gamma$ and normalized resonance strength values (with $\varepsilon_y/\pi = 1.03 \times 10^{-8}$ m) of

$$|G\gamma_n| = 4.8202, \quad |\epsilon_n|/\sqrt{\varepsilon_y/\pi} = 5.3$$

The former quantity in a good agreement with $\nu_y = 4.8201$ from the Fourier analysis of the phase space motion. The latter is in a good accord with the result obtained from the strong resonance simulation crossing, namely (Tab. 14.40, rightmost column), $|\epsilon_n|/\sqrt{\varepsilon_y/\pi} = 5.2$. The Fresnel integral model and the tracking results in the region of the resonance are superimposed in Fig. 14.19.

14.2.1.10 Beam Depolarization Using a Solenoid

A perfect Booster lattice is considered here. The integer resonance $G\gamma = -6$ is used to move initially vertical spins into the horizontal plane. Spin rotation is performed using either

- SOLENOID, in which case the magnetic field has to be provided; in addition, the solenoid is ramped from the initial to final energy in order to maintain a constant strength, which also means a constant spin tilt angle;

- SPINR, in which case the spin tilt angle, constant over the acceleration range, has to be specified; one advantage if SPINR is that it is a pure spin rotation, avoiding any possible orbit or betatron motion side effects.

Question 14.1.1.10-1 - The input data file for this simulation is given in Tab. 14.46. Note that the location of the rotator does not make a difference as the modulus of the depolarizing strength, $|\epsilon_n|$, comes in the the Froissart-Stora formula. So, for simplicity, the rotator is placed at the beginning of the optical sequence. The solenoidal field, spin tilt angle and energy range have been determined as follows.
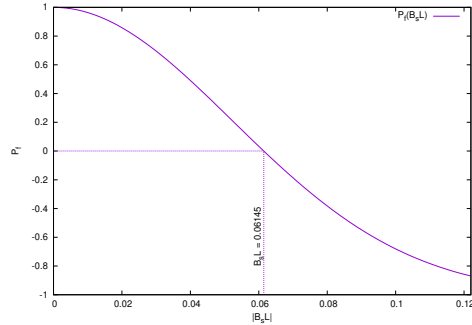
Fig. 14.20 A graph of the dependence of the final polarization on $B_s L = \int B_s(s)\,ds$ field integral (Eq. 14.9), upon crossing of the integer resonance $B\rho_n = -6$

Full depolarization after crossing $G\gamma = -6$ requires a resonance strength (Eq. 14.6 with $P_f = 0$) of

Table 14.46 Input data file for beam depolarization through $G\gamma = -6$ using a longitudinal-axis spin rotation (SOLENOID or SPINR). Note that the value of the SCALING coefficients is updated to the present initial BORO/1000=3.7764566118. SCALING ensures that power supply ramping follows the rigidity boost by CAVITE. The latter accelerates from $B\rho = 3.7764566118$ T m ($G\gamma = -5.374744555$), up to $B\rho = 5.92283102938$ T m ($G\gamma = -6.7454301$) in the asymptotic spin rotation region. The INCLUDE file here, scaling_SOLENOIDadded_Gg5.374.inc is a copy of scaling_Gg5.374.inc used in earlier exercises, with SOLENOID added

```
Depolarization by G.gamma=-6, using a longitudinal-axis rotation.
'OBJET'
3.7764566118E3 ! reference rigidity (kG.cm) at start of acceleration (G.gamma=-5.374744555).
2                                  ! Option for initial coordinates introduced individually.
1 1                                                     ! Track a single particle.
0.01 0. 0. 0.01 0. 1. 'o'          ! Small motion to check tunes (closed orbit is nul here).
1
'PARTICUL'
HELION
'SPNTRK'
3                                  ! Any particle is attributed vertical initial spin vector.
'FAISTORE'
zgoubi.fai                                      ! Log particle data in zgoubi.fai,
1                                                         ! at every pass.

         ! Scaling coefficients in scaling_GgXXX.inc are updated to present BORO/1000 value,
'INCLUDE'                                   ! SOLENOID has to be added to the list if used.
1
scaling_SOLENOIDadded_Gg5.374.inc[SCALING_S,*:SCALING_E,*]

! Two possibilities to simulate spin rotation (uncomment/comment one or the other:
! SOLENOID (give field value) or SPINR (give rotation angle).

! 'DRIFT'                                            ! Compensation for added length.
! -100.
! 'SOLENOID'
! 0
! 100. 1. 0.129      ! This field yields Bs=0.0621T at G.gamma=-6, vs. theoretical 0.0615 T
! 10. 10.                                            ! for beam depolarization.
! 1.
! 1 0. 0. 0.

'SPINR'
1
0 2.36                              ! Theoretical angle for depolarization is 2.3290 deg.
'INCLUDE'
1
6* superA.inc[superA_S:superA_E]
'CAVITE'   accelerating cavity
2
201.780048     4.00 circumf., H
400e3     0.523598775598            ! Aceleration rate is 400kV*Q*sin(30deg), Q=2.
'REBELOTE'                          ! ~19800 passes from beta=0.0655 (Ek=6.043806MeV) to
2300 0.3 99                                         ! Ggamma=-16 (Ek=7.93076082GeV).
'END'
```

$$|\epsilon_n| = \left(\frac{2\alpha}{\pi} \ln 2\right)^{1/2} = 0.0064694573$$

with the crossing speed $\alpha = 9.484842 \times 10^{-5}$ ($\hat{V} = 400$ kV, Tab. 14.46).

The theoretical solenoid field integral needed to achieve that is obtained from Eq. 2.38 with $|\epsilon_n| = 0.0064694573$ and $B\rho = B\rho_n = 4.8139470584$ T m ($G\gamma = -6$), namely

$$B_s L = \frac{2\pi B\rho_n |\epsilon_n|}{1 + G} = 0.061454684 \text{ T m}$$

The dependence of the final polarization on the field integral $B_s L$ can be expressed as (the Froissart-Stora formula)

Fig. 14.21 A graph of the SOLENOID longitudinal field $B_s(s)$ ($B_X(X)$ in Zgoubi notations) as experienced by particles in the $G\gamma \approx G\gamma_n = -6$ energy region of the acceleration ramp. The plotted data are read from zgoubi.plt. The plateau is at $\hat{B}_s = 0.0621$ T
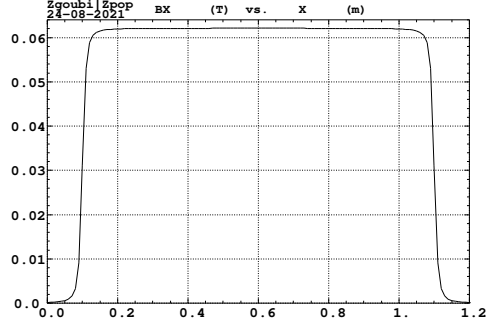
Fig. 14.22 A graph of $S_y(G\gamma)$ ($S_Z(G\gamma)$ in Zgoubi notations) through the integer resonance $G\gamma_n = -6$ excited using a 2.36 deg longitudinal-axis spin rotation. The plotted data are read from zgoubi.fai. The Outcomes of both the SOLENOID and SPINR simulation cases are super-imposed here, showing a marginal difference
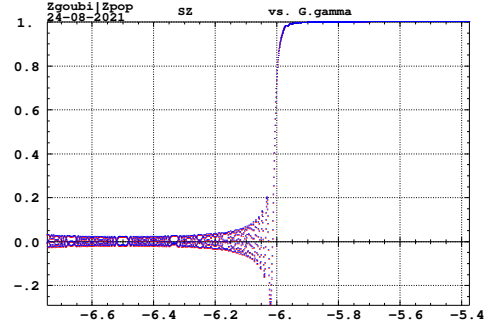
$$P_f = 2 \exp\left(-\frac{\pi}{2} \frac{\left|\frac{1+G}{2\pi B \rho_n} B_s L\right|^2}{\alpha}\right) - 1 \tag{14.9}$$

This dependence is plotted in Fig. 14.20.

The spin rotation angle is maintained constant over the acceleration range, by ramping the SOLENOID field using SCALING (Tab. 14.46). Its value is

$$\phi_{\text{sp}}(1+G)\frac{B_s L}{B\rho_n} = -0.040648 \, \text{rad} = 2.239 \, \text{deg}$$

The starting $G\gamma = -5.374744555$ is at a distance of about $100 \times |\epsilon_n|$ from the resonance, which is well away so ensuring absence of depolarizing effects. The spins stay vertical as particles circle around the ring. The final $G\gamma = -6.74543$ is about $100 \times |\epsilon_n|$ downstream of the resonance, in the asymptotic region.

In order for the spins to end up precessing about nearly longitudinal axes with the turn-average $\langle S_y \rangle_{\text{turn}} \approx 0$, the respective practical SOLENOID and SPINR settings have to be (these are the settings in the input data file given in Tab. 14.46),

$$B_s L = 0.0621 \, \text{T m, at } G\gamma = G\gamma_n, \qquad \phi_{\text{sp}} = 2.36 \, \text{deg}$$

which is reasonably close to the theoretical expectations. The longitudinal field experienced by the particles across the solenoid, when they reached the resonant energy region, is shown in Fig. 14.21.

At this point it is a good idea to ensure that coupling introduced by the solenoid is only a marginal optical perturbation (otherwise, it would have to be compensated). This can be checked with a MATRIX computation, based on the input data file of Tab. 14.46 (uncomment DRIFT and SOLENOID, comment SPINR, remove or comment CAVITE and REBELOTE, instead add MATRIX[IORD=1,IFOC=11], use OBJET[KOBJ=5], make sure SOLENOID is added to the SCALING list), yielding the following 1-turn 6 × 6 matrix:

```
   -1.09944      -5.44039     -6.570868E-03   -3.815489E-02    0.00000       0.985749
    0.355748      0.850847     2.126139E-03    6.053993E-03    0.00000      -0.271888
   -1.090396E-02  5.977518E-02  1.82449        -8.76526        0.00000       0.00000
   -1.889785E-03  6.568228E-03  0.316205       -0.971045       0.00000       0.00000
   -4.427688E-02  0.680976    -2.645957E-04    4.689973E-03    1.00000       8.97276
    0.00000       0.00000      0.00000          0.00000        0.00000       1.00000
```

It can be seen that coupling is weak. No compensation is needed in the current simulations.

The spin tracking results for the cases of both SOLENOID and SPINR are displayed in Fig. 14.22. Note that if a more accurate $B_s L$ value giving precisely $\langle S_y \rangle_{\text{turn}} = 0$ is desired, as indicated in Fig. 14.20, this can be readily achieved by a linear interpolation between a couple of tracking points near $B\rho \approx 0.61 \sim 0.62$.

Question 14.1.1.10-2 - The data file for this simulation is the same as for the previous question (Tab. 14.46) with one change: MCOBJET is used to create a 1000-particle bunch. This requires substitution of OBJET and its data list by the following:

```
'MCOBJET'
3.7764566118E3                                reference rigidity (kG.cm).
3                          ! Option to create a 6D bunch with random coordinates.
1000                                           ! A 1000-particle bunch.
2 2 2 2 2 2
0.0 0. 0. 0.0 0. 1.                            ! Mean values of the densities.
 0.982907  5.483186 1e-6  2                    ! Horizontal density parameters.
-1.545246  9.691428 1e-6  2                    ! Vertical density parameters.
 0.       1.       1.e-6 2                  ! Longitudinal density parameters.
 123456 234567 345678
```

SPINR is used to be closer to the theoretical assumptions addressed in the previous question (by avoiding possible orbital effects associated with SOLENOID). Two different 1000-particle sets have been tracked for comparison, one with $\delta p/p = 0$ which ends up with the expected $\langle S_y \rangle \approx 0$, and one with a rms Gaussian momentum spread of $\sigma_{\delta p/p} = 10^{-3}$ which ends up with $\langle S_y \rangle$ being slightly negative. The results are presented in Fig. 14.23.

14.2.1.11 Introduce a Partial Snake

Question 14.1.1.11-1 - The input data file to simulate the Booster lattice including vertical misalignment of the lattice quadrupoles (using ERRORS) and a longitudinal axis snake is given in Tab. 14.47. The snake simulation uses SPINR (a pure spin precession, no orbital effect) with the spin axis set to longitudinal and the spin precession angle ϕ_{snake} to be determined - see next question.
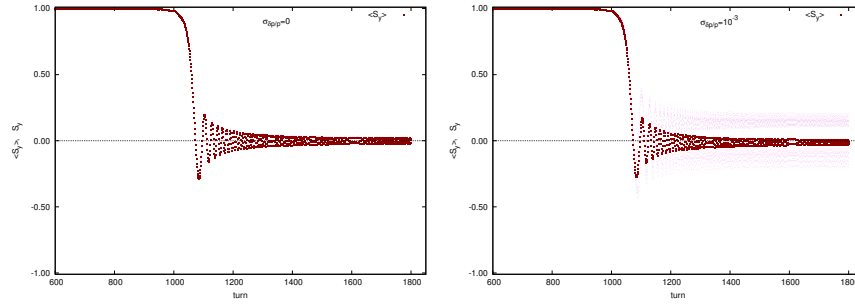
Fig. 14.23 Graphs of $\langle S_y(\text{turn}) \rangle$, an average over a 1000-particle set (dark curve), together with a few individual $S_y(\text{turn})$ taken from that random set with various ε_x, ε_y values, for the two cases (as indicated on the respective graph) of $\delta p/p = 0$ (no momentum spread) and non-zero random $\delta p/p$. Spread of the final spin vectors together with a negative offset of $\langle S_y \rangle$ is apparent in the latter case
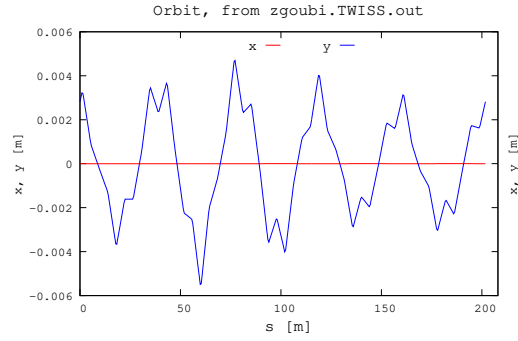
Fig. 14.24 Vertical closed orbit along Booster, with the ERRORS setting as per Tab. 14.47
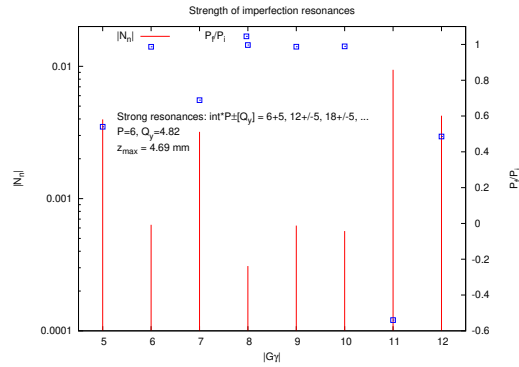
Fig. 14.25 Strengths of integer resonances excited by the orbit distortion displayed in Fig. 14.24

Integer resonances are excited by a non-zero vertical orbit. Their strengths are displayed in Fig. 14.25 over $-12 \le G\gamma \le -7$, as obtained using the thin lens model series (Eq. 2.29). Strong resonances are at $G\gamma_n = pM \pm [\nu_y] = 6 + 5 = 1$, $2 \times 6 \pm 5 = 7$, 17, etc. (with $[\nu_y] = 5$ being the nearest integer to the actual $\nu_y = 4.82$). Thus,

Table 14.47 Input data file for a simulation of an acceleration cycle in Booster in the presence of a partial snake. The latter uses SPINR. An orbit distortion is created using ERRORS, which causes a random vertical displacement of quadrupoles with an *rms* value of 0.25 mm and a 3-σ cut-off. Note that the values of the SCALING coefficients are updated to the present initial BORO/1000=5.56832079 ($G\gamma = -6.5$). SCALING ensures that power supply ramps follow the rigidity boost by CAVITE. The latter accelerates from $G\gamma = -6.5$ to $G\gamma = -10.5$ in 6500 turns

```
Partial snake to preserve polarization thru integer resonances.
'OBJET'
5.5683207908096621E3                      Reference rigidity (kG.cm) (G.gamma=-6.5, here).
2                                                              ! Launch a single
1 1                                                            ! particle, on
0. 0.    2.81903105E-01   4.05298102E-01   0.00  1. 'o'        ! closed orbit.
1
'PARTICUL'
HELION

'ERRORS'
1 1 123456 PRINT           ! sig_ZS/cm      ! PRINT logs error infos to zgoubi.ERRORS.out.
MULTIPOL{Q*,QUAD} 1 ZS A U 0.   .025    3                      ! LensFamiliy{LABEL1, LABEL2}.

'SPNTRK'
4.1                                  ! Particle spin is along stable spin axis, which is,
0. 0. 1.                             ! vertical as starting G.gamma=-6.5, away from resonance.
'FAISTORE'
zgoubi.fai                                    ! Log particle data in zgoubi.fai,
1                                             ! at every pass.

          ! Scaling coefficients in scaling_GgXXX.inc are updated to present BORO/1000 value.
'INCLUDE'
1
scaling_Gg6.5.inc[SCALING_S:SCALING_E]         ! SCALING keyword, set for G.gamma=-6.5.

'SPINR'                                  ! Snake, pur spin precession, no orbital effect.
1
0. 1.224    ! Snake axis longitudinal. Change, here, snake angle to 0, 1.224, 2.45 or 12.24.

'INCLUDE'
1
6* superA.inc[superA_S:superA_E]

'CAVITE'  accelerating cavity
2
201.780048     4.00 circumf., H
400e3     0.523598775598                    ! Aceleration rate is 400kV*Q*sin(30deg), Q=2.
'REBELOTE'                                  ! ~19800 passes from beta=0.0655 (Ek=6.043805MeV) to
6500 0.3 99                                 ! Ggamma=-16 (Ek=7.93076082GeV).
'END'
```

$G\gamma_n = 7$ is the strongest in the acceleration interval of $G\gamma : -6.5 \rightarrow -10.5$ considered in this exercise. Its theoretical strength (using Eq. 2.29) is $|\epsilon_n^{\mathrm{imp}}| = 0.0034$.

Acceleration through $G\gamma : -6.5 \rightarrow -10.5$ produces S_y(turn) displayed in Fig. 14.29 (the case of $\phi_{\mathrm{snake}} = 0$). The resonances are located at integer $G\gamma$ values separated by distant $G\Delta\gamma = 1$. Thus, in units of energy (using the particle data from Tab. 14.1),

$$\Delta E = \frac{M}{|G|}G\Delta\gamma = \frac{M}{|G|} = \frac{2808.3916}{4.18415} = 671.2 \mathrm{MeV}$$

Question 14.1.1.11-2 - The snake angle is set (under SPINR) to $\phi_{\mathrm{snake}} = 2\pi|\epsilon_n^{\mathrm{imp}}| = 2\pi \times 0.0034 \, \mathrm{rad} = 1.224°$, ERRORS is inhibited, the particle data are logged in zgoubi.fai at each optical element along the ring, the reference rigidity is set for $G\gamma = 7$ under OBJET and SCALING. The initial spin coordinates are set (to arbitrary values) under SPNTRK, and FIT is used to change them so to reach $\mathbf{S}_{x,s,y}(s = 0) = \mathbf{S}_{x,s,y}(s = s_{end})$. This yields the input data file of Tab. 14.48.

Table 14.48 Input data file to find the spin closed orbit at the $G\gamma_n = 7$ resonance (using FIT). It is similar to that of Tab. 14.47, with the following changes: the reference rigidity is BORO=6.2821070918945 ($G\gamma = 7$); ERRORS[ONF=0] inhibits the error generator; ALL is added under FAISTORE, this logs the particle data at the exits of all optical elements along the sequence in zgoubi.fai for further plotting of $\mathbf{S}_{X,Y,Z}(s)$; scaling_Gg7.inc is INCLUDEd with its scaling coefficients set for $|G\gamma| = 7$; FIT finds the periodic orbit (expected null) and the periodic spin orbit, expected to lie in the median plane due to the snake

```
Partial snake to preserve polarization thru integer resonances.
'OBJET'
6.2821070918945E3                                        reference rigidity (kG.cm).
2                               ! Option for initial coordinates introduced individually.
1 1                                                      ! Track a single particle.
0.0 0. 0. 0.0  0. 1. 'o'        ! Small motion to check tunes (closed orbit is nul here).
1
'PARTICUL'
HELION
'SPNTRK'
4.1                                    ! Particle spin is along stable spin axis, which is,
0. 1. 0.               ! arbitrarily, along the Y axis, here - FIT will move it to // X-axis.

'ERRORS'                                                 ! Inhibited, due to ONF=0.
0 1 123456 PRINT           ! sig_ZS/cm    ! PRINT logs error inofs to zgoubi.ERRORS.out.
MULTIPOL{Q*,QUAD} 1 ZS A U 0.   .025    3                      ! LensFamiliy{LABEL1, LABEL2}.

'FAISTORE'
zgoubi.fai  ALL                                         ! Log particle data in zgoubi.fai,
1                                                        ! at every pass.

        ! Scaling coefficients in scaling_GgXXX.inc are updated to present BORO/1000 value.
'INCLUDE'
1
scaling_Gg7.inc[SCALING_S:SCALING_E]                    ! SCALING keyword, set for G.gamma=-7.

'SPINR'                                 ! Snake, pur spin precession, no orbital effect.
1
0. 1.224    ! Snake axis longitudinal. Change, here, snake angle to 0, 1.224, 2.45 or 12.24.

'INCLUDE'
1
6* superA.inc[superA_S:superA_E]

'FIT2'
7
1 30 0 [-5,5]           ! First 4 lines: vary initial particle coordinates, Y, T, Z, P, iOBJET.
1 31 0 [-5,5]
1 32 0 [-5,5]
1 33 0 [-5,5]
3 10 0 [-1.01,1.01]                 ! These 3 lines: vary initial spin coordinates, SX, SY, SZ.
3 11 0 [-1.01,1.01]
3 12 0 [-1.01,1.01]
8  1e-10
3.1 1 2 #End 0. 1. 0     ! First 4 lines: request equal particle coordinates at sart and end.
3.1 1 3 #End 0. 1. 0
3.1 1 4 #End 0. 1. 0
3.1 1 5 #End 0. 1. 0
10.1 1 1 #End 0. 1. 0        ! These 3 lines: request equal spin coordinates at sart and end.
10.1 1 2 #End 0. 1. 0
10.1 1 3 #End 0. 1. 0
10   1 4 #End 1. .0001 0    ! Request spin vector modulus =1, with a great weight (0.0001).
'END'
```

The presence of the snake produces the spin closed orbit displayed in Fig. 14.26. Plotted data are read from zgoubi.fai, generated using FAISTORE[LABEL=ALL], which logs the particle data at the exits of ALL optical elements around the ring (FAISTORE[LABEL=DRIF] would probably be sufficient). The spinor methods (Chap. 3) allow for deriving the eigenvectors

$$\mathbf{n} = \begin{pmatrix} n_x \\ n_s \\ n_y \end{pmatrix} = \frac{(\pm)}{\sin \pi \nu_{sp}} \begin{pmatrix} -\sin(G\gamma(\pi - \theta)) \sin \dfrac{\phi_{snake}}{2} \\[2mm] \cos(G\gamma(\pi - \theta)) \sin \dfrac{\phi_{snake}}{2} \\[2mm] \sin(G\gamma\pi) \cos \dfrac{\phi_{snake}}{2} \end{pmatrix} \qquad (14.10)$$

and the spin tune

$$\cos \pi \nu_{sp} = \cos(\pi G\gamma) \cos(\pi \epsilon_n) = \cos(\pi G\gamma) \cos \frac{\phi_{snake}}{2} \qquad (14.11)$$

On the $G\gamma = 7$ resonance, $n_y = 0$, the spin closed orbit lies in the median plane. Figure 14.26 shows its theoretical $n_s(\theta)$ and $n_x(\theta)$ components (Eq. 14.10) superimposed on the numerical tracking results (this graph uses the gnuplot script given in Tab. 14.49). The oscillation frequency (Eq. 14.11 with $\phi_{snake} = 1.224°$) is

$$\text{frac}(\nu_{sp}) = \frac{\phi_{snake}}{2} = 0.0034$$

Table 14.49 A gnuplot script to produce the graph of the numerical and theoretical spin closed orbit vectors around the ring in Fig. 14.26. This script specifies the positions (the column numbers) of the data read from zgoubi.plt

```
set xlabel "{/Symbol q}  [rad]" ;  set ylabel "n_X,  n_Y,  n_Z"
set key t r maxrow 5   width -3

pi = 4.*atan(1.) ; deg = 180./pi ; cm = 1e2 ; am = 2808.391585; G = 4.1841538; q = 2.
R = 201.78/ (2.*pi) *cm ; qsi= 1.224/deg ; Gg = 7.

# n_0 components, theory:
SY(x) = -1./sin(acos(cos(pi*Gg)*cos(qsi/2.))) * sin( Gg* (pi -x)) * sin(qsi/2.)    # x/e1
SX(x) =  1./sin(acos(cos(pi*Gg)*cos(qsi/2.))) * cos( Gg* (pi -x)) * sin(qsi/2.)    # s/e2
SZ(x) =  1./sin(acos(cos(pi*Gg)*cos(qsi/2.))) * sin( Gg* pi) * cos(qsi/2.)         # z/e3
set sample 1000

print " Qs = ",acos(cos(pi*Gg)*cos(qsi/2.))/pi,";   1-Qs = ",1-acos(cos(pi*Gg)*cos(qsi/2.))/pi

plot [] [-1:1] \
"zgoubi.plt" u ($14/R):($33) w p pt 4 ps .4 lc rgb "red"   tit "S_X" , SX(x) lw 2. dt 2 lc rgb "red" notit ,\
"zgoubi.plt" u ($14/R):($34) w p pt 4 ps .2 lc rgb "blue"  tit "S_Y" , SY(x) lw 2. dt 3 lc rgb "blue" notit ,\
"zgoubi.plt" u ($14/R):($35) w p pt 4 ps .1 lc rgb "black" tit "S_Z" , SZ(x) lw 2. dt 4 lc rgb "black" notit
```

Question 14.1.1.11-3 - An input data file to compute the spin closed orbit for $G\gamma = 7$, using FIT, is given in Tab. 14.50. A script (as in Tab. 14.51) changes the reference rigidity (OBJET[BORO]) and the corresponding SCALING factors in the ancillary file scaling.inc, and the repeats the computation for the sampled $-G\gamma$ values over $[-6.5, -7.5]$.

Question 14.1.1.11-4 - Quadrupole misalignments are enabled (ERRORS[ONF=1]), the snake angle is set to $\phi_{snake} = 1.224°$.

Acceleration through $G\gamma : -6.5 \rightarrow -10.5$ produces $S_y(turn)$ displayed in Fig. 14.29 (the case of $\phi_{snake} = 1.224°$). The spin appears to be tilted after crossing the integer resonances. However, the snake rotation is too weak to overcome the effect of the vertical orbit distortion.

Fig. 14.26 Spin closed orbit along Booster in terms of its azimuthal angle at the $G\gamma = 7$ integer resonance. The snake is located at $\theta = 0$. The $\mathbf{n}_0$ vector lies in the median plane, and undergoes rotation about the Z-axis at a frequency of $\nu_{sp} = G\gamma$: SX (the thick red curve) and SY (blue) oscillate while SZ=0. The theoretical $\mathbf{n}_0$ vector components (Eq. 14.10) are superimposed (the dashed curves). At the azimuthal angle of $\theta = \pi$ rad, which is the location opposite to the snake, the stable spin direction vector is parallel to the longitudinal axis ($n_s \equiv$ SX = 1 and $n_x \equiv$ SY = 0)
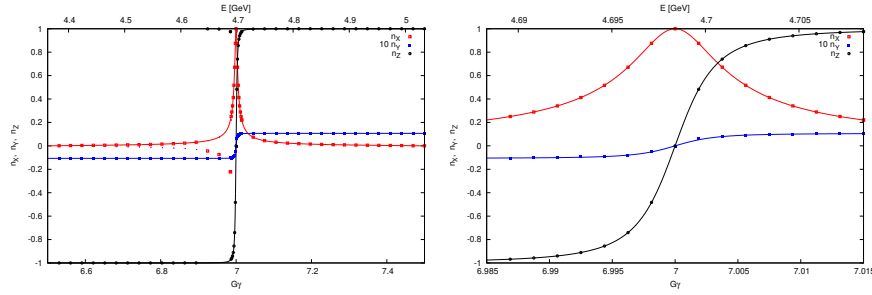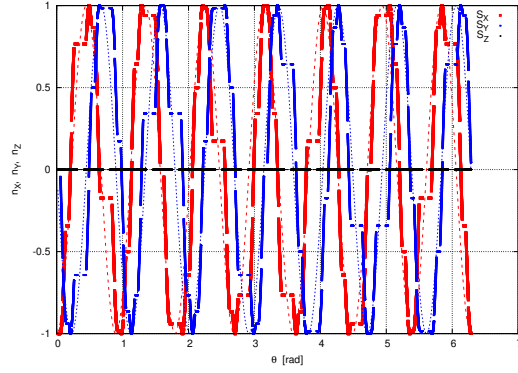
Fig. 14.27 $G\gamma$ dependence of the spin closed orbit, over $6.5 < |G\gamma| < 7.5$ (left), and a zoomed-in view of the central region (right). The symbols are from spin tracking, the solid lines are from the theory (Eq. 14.10 wherein $n_{s,x,y}$ corresponds to the present Zgoubi notation $n_{X,Y,Z}$). Note the value of the n_Y component at half-integer $G\gamma$ of $n_x \equiv n_Y = 0.01068$ enhanced by a factor 10 for accuracy (with the theoretical n_x given by Eq. 14.10)

Question 14.1.1.11-5 - In order to determine the minimum angle of the snake spin rotation, it is necessary to know the strengths of the resonances to be crossed.

A partial snake generates a spin resonance strength

$$|\epsilon^{snake}| = \frac{\phi_{snake}}{2\pi}$$

Upon crossing of the resonance, the ratio of the final and initial polarizations satisfies (the Froissart and Stora formula, Eq. 2.44)

Table 14.50 Input data file to find the spin closed orbit at a $G\gamma_n$ resonance ($G\gamma_n = 7$, here) using FIT. FIT finds the spin closed orbit for particle 4, which is $G\gamma$ dependent (Eq. 14.10). A trick is used here: the first three particles are left out of the fit, they are used to compute the spin matrix (SPNPRT[MATRIX], logged in zgoubi.SPNPRT.Out by SPNPRT[PRINT]) for comparison with the spin closed orbit of particle 4 found by FIT. Additional particles 5 and 6 are dummies and unused. They are only needed for proper operation of SPNPRT[MATRIX], which requires 3-particle subsets

```
spinN0_FIT_template.dat tmeplate input data file
'OBJET'
6.2821070918945E3                       ! Reference rigidity (kG.cm) - G.gamma=7, here.
2                                       ! Option for initial coordinates introduced individually.
6 2    ! Spin MATRIX computation requires 3 times the same particle, with spin SX, SY or SZ.
0. 0. 0. 0.  0. 1. 'o'                  ! First 3 particles used to compute spin matrix.
0. 0. 0. 0.  0. 1. 'o'
0. 0. 0. 0.  0. 1. 'o'
0. 0. 0. 0.  0. 1. 'o'                  ! 4th particle used to get spin closed orbit, using FIT.
0. 0. 0. 0.  0. 1. 'o'  ! 2 additional particles unused, only needed for proper operation of
0. 0. 0. 0.  0. 1. 'o'                  ! SPNPRT[MATRIX] as it requires 3-particle subsets.
1 1 1 1 1 1 1
'PARTICUL'
HELION
'FAISCEAU'
'SPNTRK'
4
1. 0. 0.                  ! Initial spins of first 3 particles are left untouched, used to
0. 1. 0.                                          ! compute spin matrix.
0. 0. 1.
1. 0. 0.                          ! Spin of prtcl 4 varied by FIT, to find spin orbit.
1. 0. 0.                                          ! unused.
1. 0. 0.                                          ! unused.

'INCLUDE'
1       ! scaling.inc is a cpy of scaling_Gg7.inc, scaling factors therein suited to present
scaling.inc[SCALING_S:SCALING_E]        ! OBJET[BORO] (they are changed by the repeat scrit).

'SPINR'                                 ! Snake, pur spin precession, no orbital effect.
1
0. 1.224    ! Snake axis longitudinal. Change, here, snake angle to 0, 1.224, 2.45 or 12.24.
'INCLUDE'
1
6* superA.inc[superA_S:superA_E]

'FIT2'
3
4 40 0 [-2.0,2.0]       ! These 3 lines: vary initial spin coordinates SX, SY, SZ of prtcl 4.
4 41 0 [-2.0,2.0]
4 42 0 [-2.0,2.0]
4  1e-20
10.1 4 1 #End 0. 1. 0      ! These 3 lines: request equal spin coordinates at sart and end.
10.1 4 2 #End 0. 1. 0
10.1 4 3 #End 0. 1. 0
10   4 4 #End 1. .0001 0      ! Request spin vector modulus =1, with a great weight (0.0001).

'FAISCEAU'  ! Allows to check final particle coordinates (perfect ring: should all be zero).

!    In the following: spin closed orbit from spin MATRIX (computed using particles 1-3) is
!  stored in zgoubi.SPNPRT.Out. It is expected to confirm spin closed orbit for particle 4,
!                                                   computed using FIT.
'SPNPRT' MATRIX PRINT
'END'
```

$$\frac{P_f}{P_i} = 2e^{-\frac{\pi}{2\alpha}|\epsilon^{\text{snake}} + \epsilon_n^{\text{imp}}|^2} - 1$$

Note: the overall strength $\epsilon^{\text{snake}} + \epsilon_n^{\text{imp}}$ results from a combination of the longitudinal and radial perturbative terms $\lambda_s \dfrac{B_s}{B_{y0}}$ and $\lambda_x \dfrac{B_x}{B_{y0}}$ in Eq. 2.26, with the B_s contribution coming from the snake and B_x arising from the vertical orbit in the quadrupoles.

Thus, for the snake to dominate the spin resonance dynamics, one needs

Table 14.51 A Fortran script to repeat the orbit finding of Tab. 14.50, for sampled values $G\gamma$: $-6.5 \rightarrow -7.5$. When the scan is completed, gnuplot_SPNPRT_N0-Qs-fromFIT.gnu (Tab. 14.52) is executed

```
character(300) cmnd; character(12) txt12
parameter (c = 2.99792458e8)
G = 4.1841538; am = 2808.391585; q = 2.

Gg0=6.5; N = 60

dGg = 1./float(N-1); Gg0=Gg0 -dGg
do i = 1, N
  Gg = Gg0 + dGg*float(i);  gma = Gg/G
  p = sqrt((gma*am)**2 - am**2); brho = p/c/q *1e6
  cmnd='cp -f spinN0_FIT_template.dat spinN0_FIT.dat'
  call system(cmnd)
  cmnd='cp -f spinN0_FIT_template.dat spinN0_FIT.dat'//
>   " ; sed -i 's@6.2821070918945@'//txt12//'@g' spinN0_FIT.dat"
  call system(cmnd)
  cmnd='cp -f scaling_Gg7.inc scaling.inc'//
>   "; sed -i 's@6.2821070918945@'//txt12//'@g' scaling.inc"
  call system(cmnd)
  cmnd = '/home/meot/zgoubi/SVN/current/zgoubi/zgoubi'
>   //' -in spinN0_FIT.dat ; '
>   //'/home/meot/zgoubi/current/toolbox/rzgRevision ; '
>   //'cat zgoubi.SPNPRT.Out >> zgoubi.SPNPRT.Out_cat'
  call system(cmnd)
enddo

call system('gnuplot <./gnuplot_SPNPRT_N0-Qs-fromFIT.gnu')

stop
end
```

Table 14.52 Typical gnuplot commands to obtain graphs of spin tune and spin closed orbit components from particle 4 data logged in zgoubi.SPNPRT.Out during tracking

```
# Spin tune vs. G.gamma:
am = 938.27203; G = 1.79284735

plot "zgoubi.SPNPRT.Out_cat"  u ($21==1 ? abs($18)/G*am/1e3 : 1/0):($51)  axes x2y1 w lp ps 0.6 lw 0.
pause 3

# Spin closed orbit components vs. G.gamma:
Nprtcl = 4
plot \
"zgoubi.SPNPRT.Out_cat" every 1 u ($21==Nprtcl? abs($18): 1/0):(    $13) w p pt 4 ps .6 lc rgb "red"   tit "n_Y"  ,\
"zgoubi.SPNPRT.Out_cat" every 1 u ($21==Nprtcl? abs($18): 1/0):(-10*$14) w p pt 5 ps .6 lc rgb "blue"  tit "10 n_Y" ,\
"zgoubi.SPNPRT.Out_cat" every 1 u ($21==Nprtcl? abs($18): 1/0):(    $15) w p pt 6 ps .6 lc rgb "black" tit "n_Z"
pause 3
```

$$|\epsilon^{\text{snake}}| \gg |\epsilon_n^{\text{imp}}|$$

This is qualitatively verified in Fig. 14.29, which displays motion of the spin of a particle traveling along the vertical closed orbit, while it is accelerated over $G\gamma$: $-6.5 \rightarrow -10.5$: a snake precession of $10 \times 2\pi|\epsilon_n^{\text{imp}}| = 12.2°$ allows overcoming the resonances by causing a full flip at each integer $G\gamma$ value. The lower values of $\phi_{\text{snake}} = 2\pi|\epsilon_n^{\text{imp}}| = 1.22^o$ and $\phi_{\text{snake}} = 2 \times 2\pi|\epsilon_n^{\text{imp}}| = 2.45^o$ are too weak for spin flipping.

### 14.2.1.12 Introduce Full Snakes
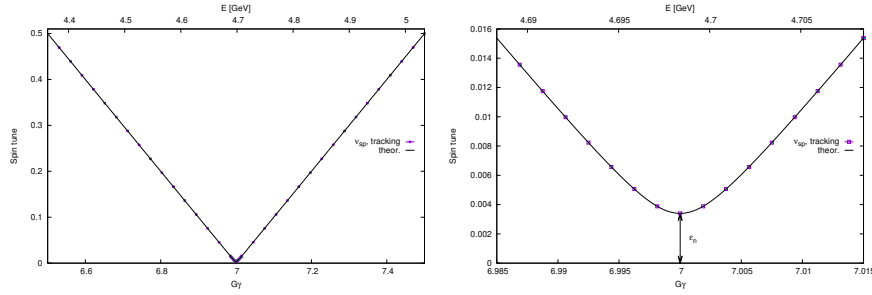
Fig. 14.28 $G\gamma$ dependence of the spin tune, over $6.5 < |G\gamma| < 7.5$, and a zoom of the central region. The symbols are from spin tracking, the solid lines are from the theory (Eq. 14.11). The width of the forbidden spin tune region, or "spin tune gap", is the resonance strength, or resonance width, $\epsilon_n = \phi_{\text{snake}}/2 = 0.0034$

Fig. 14.29 Spin motion over $G\gamma : -6.5 \rightarrow -10.5$, for the cases of 4 different snake precession angles: null, $\phi_{\text{snake}} = 2\pi|\epsilon_n^{\text{imp}}| = 1.22°$, $2 \times 2\pi|\epsilon_n^{\text{imp}}| = 2.45°$, and $10 \times 2\pi|\epsilon_n^{\text{imp}}| = 12.2°$, with $|\epsilon_n^{\text{imp}}| = 0.0034$ being the strength of the imperfection resonance excited by vertical quadrupole misalignments. The initial spin is along the vertical stable spin precession direction at $G\gamma = -6.5$
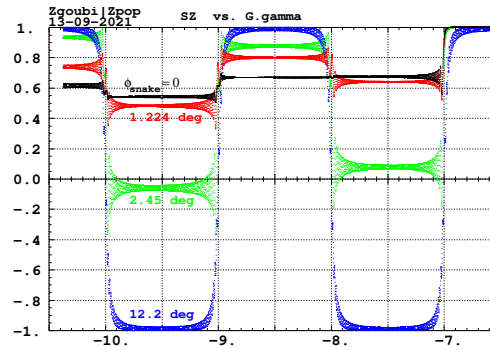
A non-zero vertical invariant is accounted for. It causes betatron motion through the lattice fields exciting systematic intrinsic spin resonances, which, given $\nu_y = 4.82$, are located at $G\gamma = -12 + \nu_y = -7.18$, $-6 - \nu_y = -10.82$, $-18 + \nu_y = -13.18$.

The same vertical closed orbit distortion as in exercise 14.2.1.11 is introduced, using ERRORS with the same data.

Question 14.1.1.12-1 - The methods here are very similar to what is done in 14.2.1.11. The spin closed orbit is found using the same input data file (Tab. 14.48). The FIT procedure in that file simultaneously finds the particle closed obit (x_0, x'_0, y_0, y'_0) ((Y_0, T_0, Z_0, p_0) in Zgoubi notation), and the spin closed orbit (which by definition is that of the particle on closed orbit). Thus, that FIT procedure holds for chromatic closed orbits. All that needs be changed is the particle D value (relative momentum) under OBJET. The closed orbits of interest here are detailed below.

The one-turn spin matrix, and thus the spin tune, the local spin precession axis at the start of the sequence, etc., can be computed using SPNPRT[MATRIX]. Computation of the spin matrix at different momenta requires defining groups of momenta, using OBJET[KOBJ=2,IDMAX=3]. The input data file used is given in

Table 14.53 Input data file to compute the one-turn spin matrices for 3 different momenta, $D = p/p_0 = 1,\ 1.0001,\ 1.001$. In order to produce the respective matrices, SPNPRT[MATRIX] requires defining 3 groups of momenta in the proper order. This can be achieved using OB-JET[KOBJ=2,IDMAX=3]. The same particle coordinates are repeated three times in each group. Then SPNTRK sets the three initial spin vectors to (1,0,0), (0,1,0), and (0,0,1), respectively

```
Full snake to preserve polarization thru integer resonances.
'OBJET'
5.5683207908096621E3                    Reference rigidity (kG.cm) (G.gamma=-6.5, here).
2
9 3                                                 ! 9 particles, 3 different momenta.
0. 0.  2.81903105E-01 4.05298102E-01  0.  1. 'o'      ! On-momentum closed orbit, dp/p=0.
0. 0.  2.81903105E-01 4.05298102E-01  0.  1. 'o'
0. 0.  2.81903105E-01 4.05298102E-01  0.  1. 'o'
7.4360716E-03 -1.0564233E-02 0.2809611 0.4040692  0.  1.0001 'd'  ! closed orbit, dp/p=1e4.
7.4360716E-03 -1.0564233E-02 0.2809611 0.4040692  0.  1.0001 'd'
7.4360716E-03 -1.0564233E-02 0.2809611 0.4040692  0.  1.0001 'd'
7.4744578E-02 -0.1053352 0.2727098 0.3932872 0.  1.001 'd'        ! closed orbit, dp/p=1e3.
7.4744578E-02 -0.1053352 0.2727098 0.3932872 0.  1.001 'd'
7.4744578E-02 -0.1053352 0.2727098 0.3932872 0.  1.001 'd'
1 1 1 1 1 1 1 1 1
'PARTICUL'
HELION
'ERRORS'
1 1 123456 PRINT          ! sig_ZS/cm        ! Vertical alignment random error, uniform.
MULTIPOL{Q*,QUAD} 1 ZS A U 0.   .025     3                   ! LensFamiliy{LABEL1, LABEL2}.
'SPNTRK'
4                                        ! SX, SY, SZ spin values of the 3*3 particles.
1. 0. 0.
0. 1. 0.
0. 0. 1.
1. 0. 0.
0. 1. 0.
0. 0. 1.
1. 0. 0.
0. 1. 0.
0. 0. 1.

'FAISTORE'
zgoubi.fai                                      ! Log particle data in zgoubi.fai,
1                                               ! at every pass.

       ! Scaling coefficients in scaling_GgXXX.inc are updated to present BORO/1000 value.
'INCLUDE'
1
scaling_Gg6.5.inc[SCALING_S:SCALING_E]           ! SCALING keyword, set for G.gamma=-6.5.

'SPINR'
1
0. 180.                                 ! Snake axis longitudinal. Full snake.

'INCLUDE'                                               ! Include Booster ring.
1
6* superA.inc[superA_S:superA_E]

'FAISCEAU'
'SPNPRT' MATRIX

'END'
```

Tab. 14.53. It defines 3 respective groups of $D - 1 = dp/p_0 = 0,\ 10^{-4},\ 10^{-3},\ 10^{-2}$. SPNPRT[MATRIX] manages that information and produces the corresponding 3 one-turn spin matrices. Excerpts from zgoubi.res given in Tab. 14.54 detail the momentum dependence of the numerical parameter values. At $G\gamma = -6.5$, the spin closed orbit at the snake is along the transverse horizontal axis, and is longitudinal at the azimuthal angle opposite to the snake, as seen in the following excerpts from zgoubi.res:

- at the snake (s=0.57 m, the end of the first drift, element number 12 in the optical sequence):

```
        12  Keyword, label(s) :  DRIFT      DRIF           L057
```

Table 14.54 SPNPRT[MATRIX] listing in zgoubi.res (excerpts): one-turn spin matrices and other information, at relative momenta $D - 1 = dp/p_0 = 0,\ 10^{-4},\ 10^{-3},\ 10^{-2}$

```
                        --------------------------------------------------------------------------
                        Momentum  group  #1 (D=  1.000000E+00) ; average  over 3 particles at this pass :

                        Spin transfer matrix, momentum group # 1 :
            -0.999945         8.562650E-06   -1.050193E-02
             6.942346E-05     0.999983       -5.794851E-03
             1.050171E-02    -5.795260E-03   -0.999928

    Trace =      -0.9998897078,    ;   spin precession acos((trace-1)/2) =    179.3982765528 deg
    Precession axis : (-0.0000, -1.0000,  0.0029) -> angle to (X,Y) plane, angle to X axis :  0.1660,  90.3855  degree
    Spin tune  Qs (fractional) :     0.49833

                        --------------------------------------------------------------------------
                        Momentum  group  #2 (D=  1.000100E+00) ; average  over 3 particles at this pass :

                        Spin transfer matrix, momentum group # 2 :
            -0.999943        -2.383130E-03   -1.045329E-02
            -2.322598E-03     0.999980       -5.799063E-03
             1.046690E-02    -5.774451E-03   -0.999929

    Trace =      -0.9998905823,    ;   spin precession acos((trace-1)/2) =    179.4006668061 deg
    Precession axis : ( 0.0012, -1.0000,  0.0029) -> angle to (X,Y) plane, angle to X axis :  0.1658,  67.8736  degree
    Spin  tune  Qs (fractional) :     0.49834

                        --------------------------------------------------------------------------
                        Momentum  group  #3 (D=  1.001000E+00) ; average  over 3 particles at this pass :

                        Spin transfer matrix, momentum group # 3 :
            -0.999664        -2.391167E-02   -1.002755E-02
            -2.385398E-02     0.999698       -5.834018E-03
             1.016403E-02    -5.592859E-03   -0.999933

    Trace =      -0.9998980571,    ;   spin precession acos((trace-1)/2) =    179.4215005685 deg
    Precession axis : ( 0.0119, -0.9999,  0.0029) -> angle to (X,Y) plane, angle to X axis :  0.1637,  13.4539  degree
    Spin  tune  Qs (fractional) :     0.49839

                        --------------------------------------------------------------------------
                        Momentum  group  #4 (D=  1.010000E+00) ; average  over 3 particles at this pass :

                        Spin transfer matrix, momentum group # 4 :
            -0.971396        -0.237373       -6.677918E-03
            -0.237335         0.971409       -5.970173E-03
             7.904151E-03    -4.214493E-03   -0.999960

    Trace =      -0.9999460691,    ;   spin precession acos((trace-1)/2) =    179.5792323606 deg
    Precession axis : ( 0.1195, -0.9928,  0.0026) -> angle to (X,Y) plane, angle to X axis :  0.1469,   1.2291  degree
    Spin  tune  Qs (fractional) :     0.49883




                                    Drift,  length =    57.04000   cm
          TRAJ #1 IEX,D,Y,T,Z,P,S,time :  1  0.   0.  0.   3.050213E-01  4.052981E-01  5.7040005E+01  2.48626E-03
          TRAJ #1 SX, SY, SZ, |S| :  1   1.962212E-05  -9.999958E-01   2.897616E-03   1.000000E+00
           Cumulative length of optical axis =   0.5704 m   ;  Time (for reference rigidity & particle) =  2.486264E-09 s
```

- at the azimuthal location opposite to the snake (s=100.9 m away, element number 330 in the optical sequence):

```
          330 Keyword, label(s) :  DRIFT      DRIF              L057
                                    Drift,  length =    57.04000   cm
          TRAJ #1 IEX,D,Y,T,Z,P,S,time :  1  0.   2.708E-05 -5.847E-05 -3.839713E-01 -3.940313E-01  1.0146044E+04  4.42247E-01
          TRAJ #1 SX, SY, SZ, |S| :  1   9.999388E-01  -1.416886E-05   1.106666E-02   1.000000E+00
           Cumulative length of optical axis =    101.460424 m ;  Time (for reference rigidity & particle) =  4.422465E-07 s
```

Question 14.1.1.12-2 - Acceleration over $G\gamma : -6.5 \rightarrow -13.5$ uses the input data file given in Tab. 14.55. It is similar to that of Tab. 14.47 but with OBJET[KOBJ=8] to generate a few particles on a matched ellipse with a given invariant (to study the dependence of the spin motion on the betatron motion), and with the number of turns increased to 11750 under REBELOTE so to reach $G\gamma = -13.5$.

Table 14.55 Input data file for a simulation of an acceleration cycle in Booster in the presence of a single full snake. The latter implemented using SPINR. An orbit distortion is created using ERRORS, which causes random vertical displacements of the quadrupoles with an *rms* value 0.25 mm and a 3-σ cut-off. Note that the values of the SCALING coefficients are updated to the present initial BORO/1000=5.56832079 ($G\gamma = -6.5$). SCALING ensures that power supply ramps follow the rigidity boost by CAVITE. The latter accelerates from $G\gamma = -6.5$ to $G\gamma = -13.5$ in 11700 turns. The initial coordinates are taken on a matched ellipse with a normalized $\varepsilon_y = 2.5\,\pi\mu$m

```
Full snake to preserve polarization thru integer resonances.
'OBJET'
5.5683207908096621E3                      Reference rigidity (kG.cm) (G.gamma=-6.5, here).
8
1 3 1
0. 0.   2.81903105E-03  4.05298102E-04  0.00  1. 'o'                   ! closed orbit.
 0.982907  5.483186  0.
-1.545246  9.691428  3.e-6         ! Vertical invariant value is 2.5 pi.mu_m, normalized.
 0. 1. 0.
'PARTICUL'
HELION
'ERRORS'
1 1 123456 PRINT           ! sig_ZS/cm        ! Vertical alignment random error, uniform.
MULTIPOL{Q*,QUAD} 1 ZS A U 0.   .025     3                ! LensFamiliy{LABEL1, LABEL2}.
'SPNTRK'
4.1
0. 1. 0.                                                  ! Initial particle spins.

'FAISTORE'
zgoubi.fai                                 ! Log particle data in zgoubi.fai,
1                                                        ! at every pass.

        ! Scaling coefficients in scaling_GgXXX.inc are updated to present BORO/1000 value.
'INCLUDE'
1
scaling_Gg6.5.inc[SCALING_S:SCALING_E]          ! SCALING keyword, set for G.gamma=-6.5.
'SPINR'
1
0. 180.                                    ! Snake axis longitudinal. Full snake.

'INCLUDE'                                                ! Booster lattice.
1
6* superA.inc[superA_S:superA_E]

'CAVITE'   accelerating cavity
2
201.780048      4.00 circumf., H
400e3     0.523598775598            ! Aceleration rate is 400kV*Q*sin(30deg), Q=2.
'REBELOTE'                          ! ~19800 passes from beta=0.0655 (Ek=6.043805MeV) to
11750 0.3 99                        ! Ggamma=-16 (Ek=7.93076082GeV).

'FAISCEAU'                                 ! Log local particle data to zgoubi.res.
'SPNPRT'                                   ! Log local spin data to zgoubi.res.
'END'
```

The results are displayed in Fig. 14.30. The initial spins are along the transverse horizontal axis (Y, in Zgoubi notation), which is the orientation of the local spin closed orbit. No polarization loss is observed: the spins exhibit stable precession about the vertical axis (Z), turn after turn.

Question 14.1.1.12-3 - Horizontal motion is added: 9 particles are launched with normalized $\varepsilon_x = \varepsilon_y = 2.5\,\pi\mu$m and 9 combinations of the initial betatron phases, by *ad hoc* modification of OBJET[KOBJ=8]:

```
'OBJET'
5.5683207908096621E3                      Reference rigidity (kG.cm) (G.gamma=-6.5, here).
8
3 3 1
0. 0.   2.81903105E-03  4.05298102E-04  0.00  1. 'o'                   ! closed orbit.
 0.982907  5.483186  3.e-6
-1.545246  9.691428  3.e-6         ! Vertical invariant value is 2.5 pi.mu_m, normalized.
 0. 1. 0.
```
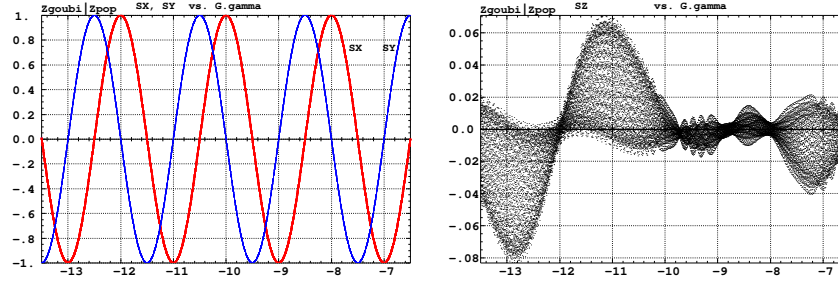
Fig. 14.30 Rotational spin motion as observed at the snake (the mid-plane components S_X and S_Y versus $G\gamma$) (left), and the (marginal) vertical component (S_Z versus $G\gamma$) (right), during acceleration over $G\gamma : -6.5 \rightarrow -13.5$, in the presence of a single full snake. Three particles are tracked, with different initial betatron phase advances on the same matched phase-space ellipse with a normalized invariant $\varepsilon_Y = 2.5\,\pi\mu$m. Their spin trajectories overlap. The initial spins are along the Y axis corresponding to the local spin closed orbit at $G\gamma = -6.5$

The results are essentially unchanged. Motion of the spins is similar to that in Fig. 14.30 found earlier.

14.2.1.13 Preserve Polarization Using Tune Jump

Question 14.1.1.15-1 - For a 100 kV RF voltage the crossing speed is

$$\frac{dG\gamma}{d\theta} = 2.37121051717 \times 10^{-5}$$

Given the tune $\nu_Z = 0.82$, the acceleration rate and the energy at the start of the tracking, the resonance $|G\gamma| = 0 + \nu_Z$ occurs at a turn number

$$N_{0+\nu_y} \approx 1530$$

The resonance strength ϵ_n is in question. It can be determined from the particle invariant using Tab. 14.40. Given ϵ_n and the crossing speed $\alpha = \frac{dG\gamma}{d\theta}$, the Froissart-Stora formula (Eq. 2.44) yields the expected asymptotic polarization after crossing of

$$P_f \approx 0.53$$

A numerical simulation of this resonance crossing yields the result displayed in Fig. 14.31 and confirms the expected $P_f \approx 0.53$.
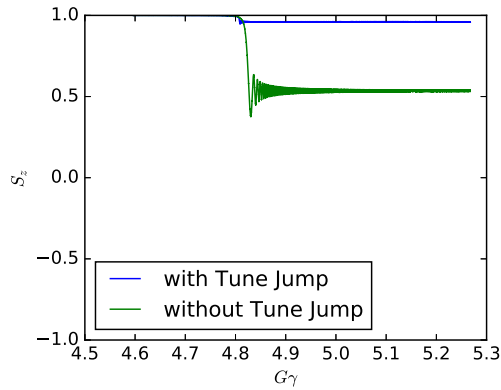
Fig. 14.31 Evolution of the polarization component $S_y(G\gamma)$ of helions when crossing the $|G\gamma| = 0 + \nu_Z$ resonance, with and without use of the tune jump quadrupoles. The plotted turn-by-turn data are read from zgoubi.fai

Question 14.1.1.15-2 - The new crossing speed, including the effect of the tune jump, is (Eq. 14.2)

$$\alpha = 2.60504500631 \times 10^{-4}$$

With this increased crossing speed, the Froissart-Stora formula yields an expected final polarization of

$$P_f = 0.9234742$$

This theoretical value agrees with the value obtained from a crossing simulation within 0.03%. The result of the latter is displayed in Fig. 14.31.

14.2.1.14 Preserve Polarization Using an AC Dipole

With the scale_factor set to 0.0, tracking a 32 particle set yields an average $P_f = 41.5\%$, compared to the expectation of $P_f = 40.0\%$.

With the scale factor set to 5 G, tracking the 32 particle set yields $P_f = -50\%$.

An AC dipole field of $B_m = 12.2\,\mathrm{G}$ allows a full spin-flip.

The tracking results are displayed in Fig. 14.32.
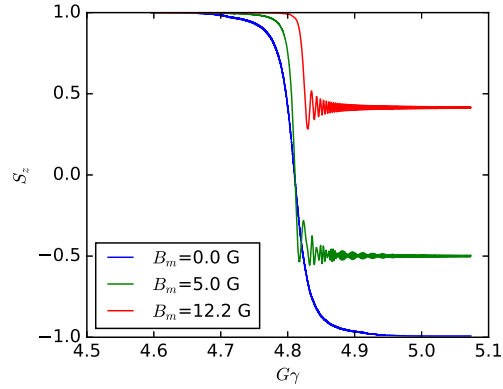
Fig. 14.32 Helions crossing the $|G\gamma| = 0 + \nu_Z$ resonance, with an AC dipole operating at $B_m = 5$ and 12.2 G. Crossing without the AC dipole (the $B_m = 0$ case) is shown for comparison. The plotted turn-by-turn data are read from zgoubi.fai

14.2.2 Electron Spin Dynamics, Synchrotron Radiation

14.2.2.1 Electron Equilibrium Emittances and Energy Spread

Question 14.1.2.1-1 - Figure 14.33 shows the optical functions and the orbit of a perfectly aligned AGS Booster ring. It was generated by a Gnuplot script (Tab. 14.14) using the Zgoubi Twiss output following the question's instructions in Sec. 14.1.2.1. The Twiss output file contains a table of the Twiss functions specified at the end of each element in the lattice. An easy way to find the damped equilibrium emittances, energy spread and damping times of 10 GeV electrons in this lattice is to open the output text file in a spreadsheet and then evaluate the integrals in the expressions for the equilibrium parameters given in Chap. 6. We can calculate approximate integral values by summing the integrand expressions over all elements. This is an accurate approximation in our case, since the Twiss functions do not change significantly over a single element. The resulting equilibrium parameters are summarized in Tab. 14.56.
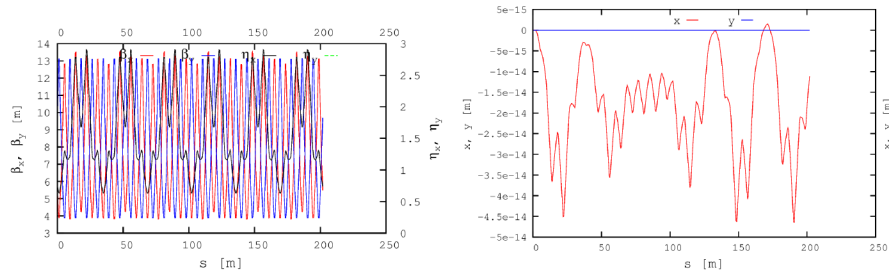
Fig. 14.33 Left: Twiss optical functions of the entire AGS Booster ring. Right: Orbit in the AGS Booster ring with perfect element alignment

Table 14.56 Electron beam parameters

Parameter	Units	Value
E, total	[GeV]	10
$a\gamma$		22.6938
Energy loss per turn	[MeV]	63.8
RF voltage	[MV]	127.6
RF phase	[rad]	2.618
Harmonic number		100
RF frequency	[MHz]	1.487
Horizontal damping time	[ms]	0.235
Vertical damping time	[ms]	0.211
Longitudinal damping time	[ms]	0.100
Horizontal emittance	[μrad]	4.53
Energy spread	$\times 10^{-3}$	2.24

Question 14.1.2.1-2 - The SRPRNT keyword at the end of the code in Tab. 14.16 activates printout of the SR loss statistics in zgoubi.res output file. An excerpt of zgoubi.res file showing the SR information is:

```
* Monte Carlo S.R. statistics, from beginning of structure,
      10000 particles,  a total of      87840762 integration steps :
   Average energy loss per particle per pass :      63968.01    keV.       Relative to initial energy :  6.3968014E-03
   Critical energy of photons (average) :           158.9614    keV
   Average energy of radiated photon :              49.30345    keV
   rms energy of radiated photons :                 92.27650    keV
   Smallest, BIGEST photon :               0.0000E+00      9.9915E+03    keV
   Number of photons radiated - Total :                      1.2974348E+07
                              - per particle per pass :         1297.435
                              - per particle, per step :        0.1477030
```

As one can see, the average particle energy loss per turn obtained in the Monte-Carlo simulation is in a good agreement with the theoretical prediction in Tab. 14.56. One must restore this energy loss at a synchronous phase necessary for longitudinal stability. Therefore, the cavity voltage amplitude is $|\hat{V}| = \Delta E/q/\sin\phi_s = 127.6\,\text{MV}$. This number is consistent with the rf cavity setting under CAVITE in Tab. 14.17, namely $\hat{V} = 122.345\,\text{MV}$. The cavity setting is slightly lower than the theoretical prediction because it accounts for the change in the particle energy as it moves around the ring.

Question 14.1.2.1-3 - The initial beam distribution in Tab. 14.17 is generated on a matched vertical phase-space ellipse, using OBJET[KOBJ=8]. The ellipse parameters are specified by the appropriate option of the OBJET element using the Twiss functions at the start point and the beam emittances. The matched Twiss function values were taken from the Twiss table that was generated as a result of Question 14.1.2.1-1. For simplicity, the horizontal and vertical emittances (noting that $\varepsilon_{x,y} = \sigma_{x,y}^2/\beta_{x,y}$, as usual in electron machines) were set to zero while the vertical emittance was set to a relatively large value of $10\,\mu$rad for synchrotron damping demonstration. After running the simulation and analyzing, plotting and fitting the resulting data as described by the question's statement in Sec. 14.1.2.1, we obtain evolution of the vertical beam emittance as a function of the turn number shown in Fig. 14.34. The vertical emittance ε_y is obtained from the rms beam size σ_y as $\varepsilon_y = \sigma_y^2/\beta_y$.

An exponential fit to the simulation data in Fig. 14.34 gives a vertical emittance damping time of 155.3 turns. Note that the equations of Chap. 6 and the values listed in Tab. 14.56 are for the amplitude damping times rather than the emittance ones. Since the emittance is proportional to the second power of the betatron amplitude, the vertical betatron amplitude damping time is a factor of two longer than the vertical emittance one and equals 310.6 turns. Given the electron circulation frequency in the AGS Booster listed in Tab. 14.56, this number corresponds to 0.209 ms, which is in a good agreement with the theoretical prediction of 0.211 ms in Tab. 14.56.

Fig. 14.34 Damping of the vertical emittance of a 10 GeV electron beam in the AGS Booster lattice. Note a good agreement of the exponential fit with the Monte-Carlo data for only 100 electrons
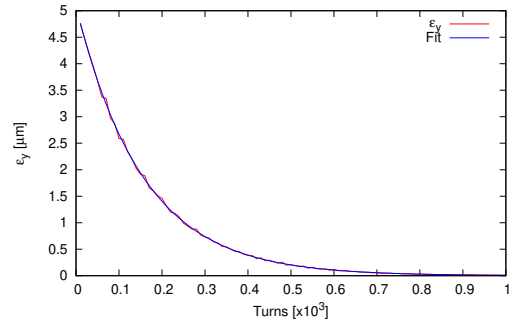
14.2.2.2 Spin Diffusion Studies

14.2.2.3 Spin Diffusion

Question 14.1.2.2-1 - Here is an excerpt of zgoubi.res file showing the spin transfer matrix, n_0 and spin tune:

```
        Spin transfer matrix, momentum group # 1 :

      -0.345661      -0.938359       0.00000
       0.938359      -0.345661       0.00000
       0.00000        0.00000        1.00000

Trace =     0.3086770996,    ;   spin precession acos((trace-1)/2) =    110.2221783671 deg
Precession axis :  ( 0.0000,  0.0000,  1.0000)  ->  angle to (X,Y) plane,  angle to X axis :   90.000,  90.000 degree
Spin  tune  Qs (fractional) :     3.0617E-01
```

As one can see, in a perfectly aligned lattice, n_0 is exactly vertical.

Question 14.1.2.2-2 - The electron polarization is plotted against the turn number in Fig. 14.35. It was obtained by tracking 100 electrons through a perfectly aligned AGS Booster lattice with synchrotron radiation enabled. At the start, the electron spins were set along the n_0 axis. Figure 14.35 illustrates that in a perfectly aligned ring, there is no detectable polarization degradation on this time scale even when synchrotron radiation is present, i.e. the spin diffusion rate is zero within our numerical precision. This case presents interest primarily as a sanity check of the spin tracking code. It confirms that at this level, the code does not introduce unphysical spin effects.

Fig. 14.35 Polarization of 100 electrons as a function of the turn number in a perfectly aligned AGS Booster ring with synchrotron radiation enabled. The electron spins are initially aligned with the n_0 axis
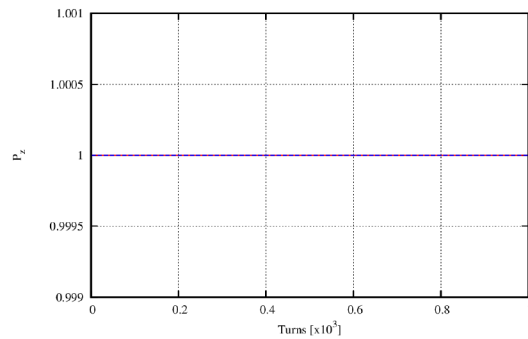
Question 14.1.2.2-3 - The 4D transverse closed orbit offset $(Y\ T\ Z\ P)$ caused by a 1 mm vertical misalignment of the "QVA1" quadrupole is

```
-5.78398841E-06  -5.02369232E-06  -2.40168827E-01  -5.80016582E-01
```

The n_0 axis at the beginning of this perturbed lattice is

```
(0.0137, -0.0568,  0.9983)
```

Time evolution of the polarization in this case is compared to that of the perfectly aligned case of Question 14.1.2.2-2 in Fig. 14.36. An exponential fit to the data gives a spin diffusion time of $17.9 \cdot 10^3$ turns corresponding to 12 ms. Note the rapid spin diffusion caused by misalignment of even a single element.
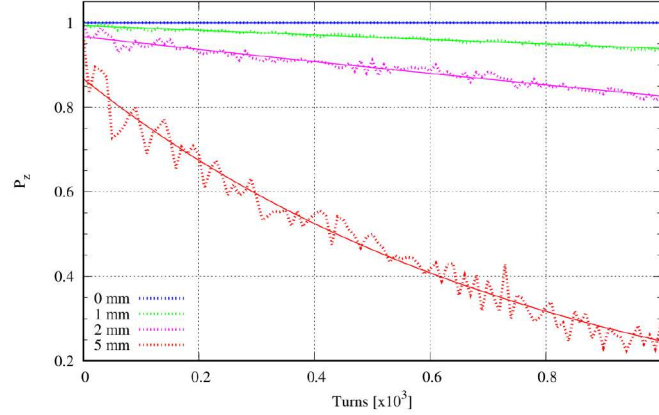
Fig. 14.36 Polarization of 100 electrons as a function of the turn number in the AGS Booster lattice for 0, 1, 2, and 5 mm vertical offsets of the first "QVA1" quadrupole. Synchrotron radiation is enabled. The electron spins in each case are initially aligned with the corresponding $\mathbf{n}_0$ axis

Question 14.1.2.2-4 - Similarly to the solution of Question 14.1.2.2-3, we find that vertical misalignments of "QVA1" by 2 and 5 mm result in transverse closed orbit shifts of

```
-2.41767056E-05    3.83288439E-05   -4.80358495E-01   -1.16006824E+00
```

and

```
-1.49937996E-04    1.83685654E-04   -1.20099981E+00   -2.90035565E+00 ,
```

respectively. The corresponding $\mathbf{n}_0$ axes are

```
(0.0273, -0.1132,  0.9932)
```

and

```
(0.0660, -0.2769,  0.9586) .
```

Note that the closed orbit offset and the x and y components of $\mathbf{n}_0$ scale linearly with the size of the misalignment as expected. The polarization behavior in these two cases is plotted as a function of the turn number in Fig. 14.36. Exponential fits to these data give spin diffusion times of $6.4 \cdot 10^3$ and 800 turns, or 4.3 and 0.54 ms, for the 2 and 5 mm misalignment scenarios, respectively.

In a perfectly aligned lattice without transverse coupling, particles with different momentum offsets δ experience only vertical bending and focusing magnetic fields. Therefore, the precession axes of all particles $\mathbf{n}(\delta)$ are aligned with the same vertical $\mathbf{n}_0$ axis. Change in momentum of a particle due to emission of a synchrotron radiation photon does not change the direction of its $\mathbf{n}(\delta)$ and causes no polarization loss as illustrated by Question 14.1.2.2-2. In case when the closed orbit experiences vertical excursion, the radial fields of the focusing quadrupoles tilt $\mathbf{n}_0$ from the vertical. The amount of this tilt is momentum dependent thus resulting in a spread of the $\mathbf{n}(\delta)$ directions for different δ. Emission of a synchrotron radiation photon changes the direction of $\mathbf{n}(\delta)$ and only the component of the original spin direction along the new $\mathbf{n}(\delta)$ is preserved. The greater the change in $\mathbf{n}(\delta)$, the smaller the fraction of the spin

that is preserved and thus the higher the spin diffusion rate. Greater misalignments lead to greater closed orbit distortion and subsequently greater deviation of $\mathbf{n}_0$ from the vertical, greater $\mathbf{n}(\delta)$ spread and finally greater spin diffusion rate as demonstrated in Question 14.1.2.2-4.

14.2.2.4 Suppression of Spin Diffusion

Question 14.1.2.2-5 - Both lattices considered in this exercise consist of a solenoid followed by two dipoles and then another solenoid. Both schemes are simplified versions of an electron spin rotator, a device rotating the electron polarization from vertical to longitudinal and then back. Such an insertion is needed to provide longitudinal polarization in the experimental section without causing fast spin diffusion in the arcs. The first solenoid rotates the polarization about the longitudinal axis from positive vertical to positive radial. The subsequent dipole rotates the polarization about the vertical axis from positive radial to positive longitudinal. The difference between the two schemes is in how the polarization is returned back to positive vertical. In the first scenario, the second dipole bends the beam in the same direction as the first one and continues polarization rotation in the same direction from positive longitudinal to negative radial. The second solenoid has the same field polarity as the first one. It rotates the polarization from negative radial to positive vertical. This dynamics can be graphically summarized as

$$\uparrow \text{ Solenoid } \odot \text{ Dipole } \rightarrow \text{ Dipole } \otimes \text{ Solenoid } \uparrow . \qquad (14.12)$$

In the second scenario, the polarities of the second dipole and solenoid are reversed resulting in the following rotation sequence

$$\uparrow \text{ Solenoid } \odot \text{ Dipole } \rightarrow \text{ Anti} - \text{Dipole } \odot \text{ Anti} - \text{Solenoid } \uparrow . \qquad (14.13)$$

In both cases, the polarization is positive vertical at the entrance and exit. From geometrical point of view, the first arrangement causes 138.4 mrad net orbital bend while the second configuration has zero net bend.

Question 14.1.2.2-6 - The field and spin components along the reference trajectories of the two spin rotator configurations are shown in Figs. 14.37 and 14.38, respectively. These graphs demonstrate implementation of the design philosophy described in the solution to Question 14.1.2.2-5.

Question 14.1.2.2-7 - Figure 14.39 shows the electron vertical spin component at the end of the spin rotator as a function of the particle's relative momentum offset. The momentum dependencies are compared for the two spin rotator configurations. In this study, different-momentum electrons with initially vertical spins were launched on the design orbit at the beginning of the spin rotator and tracked to its end. As we can see, the spin effects of the two rotator designs are equivalent for the on-momentum particles resulting in a perfect restoration of the vertical spin at the
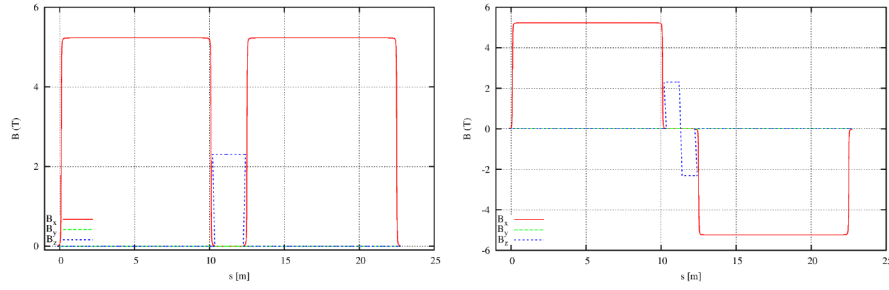
Fig. 14.37 Left: Field components along the reference trajectory in the same-field-polarity design. Right: Field components along the reference trajectory in the reversed-field-polarity design
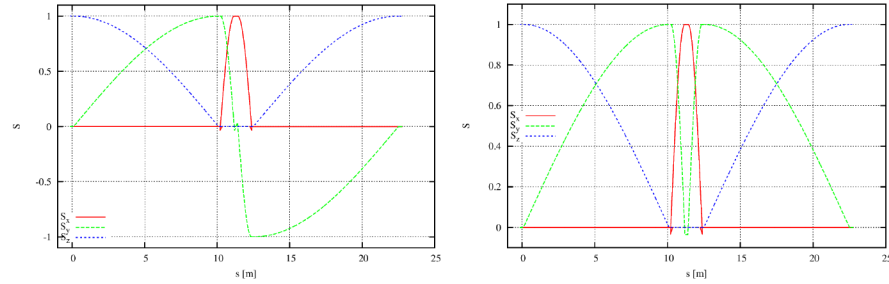
Fig. 14.38 Left: Spin components along the reference trajectory in the same-field-polarity design. Right: Spin components along the reference trajectory in the reversed-field-polarity design

end. However, there are significant differences for the off-momentum particles. The reversed-field-polarity design demonstrates a much weaker momentum dependence of the final spin. The remaining dependence is due to dispersion that has not been accounted for in this simplified scheme.
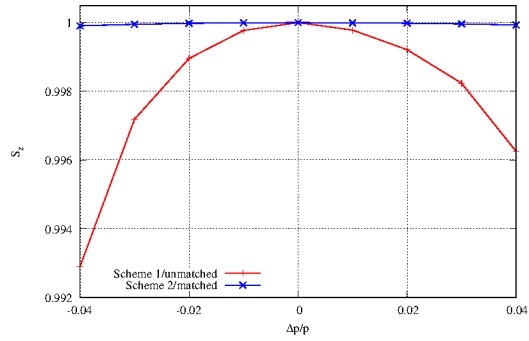
Fig. 14.39 Final vertical spin component as a function of the particle's relative momentum offset for the same-field- (Scheme 1) and reversed-field-polarity (Scheme 2) spin rotator configurations

The spin precession in each of the spin rotator elements is of course momentum dependent. The spin rotation of an off-momentum electron deviates from that of the

reference particle. In the same-field-polarity configuration, this deviation accumulates from magnet to magnet resulting in a relatively large tilt of the spin at the end. In the opposite-field-polarity configuration, the spin deviation accumulated in the first half of the spin rotator is precisely compensated by the matching opposite-field magnets in the second half causing equal-size opposite-direction spin rotations. As we demonstrated in the solution to Question 14.1.2.2-4, greater deviation of the spin from vertical in the arcs results in a higher spin diffusion rate. Therefore, the same-field-polarity configuration is expected to generate a much higher spin diffusion rate than the opposite-field-polarity one. The opposite-field-polarity design is an illustration of the concept of first-order longitudinal spin matching.

14.2.2.5 Spin Matching

Question 14.1.2.5-1 - The snake lattice in Tab. 14.33 is close to an identity transformation in the horizontal plane and a $-I$ transformation in the vertical plane. Therefore, its insertion into the AGS Booster lattice results in a reasonable periodic solution not requiring any rematch. For simplicity, we ignore the fact that the ring is no longer geometrically closed, since this does not alter the below general conclusions about the spin dynamics. The optics of the entire ring and an expanded view of the snake section are shown in Figs. 14.40(left) and (right), respectively.
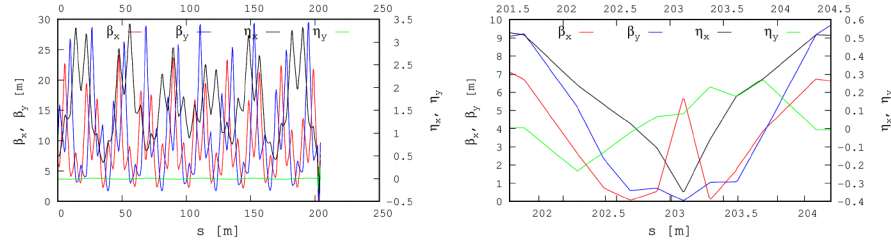
Fig. 14.40 Left: Optics of the AGS Booster ring with the spin-matched snake insertion. Right: Expanded view of the optics of the spin-matched snake insertion

Question 14.1.2.5-2: The n_0 axis at the start of the AGS Booster lattice with the solenoidal snake (Tab. 14.35) can be found in the following excerpt of zgoubi.res:

```
               Spin transfer matrix, momentum group # 1 :

        -0.571992      0.820259       8.558277E-14
         0.820258      0.571991      -1.676874E-03
        -1.375471E-03 -9.591582E-04  -0.999999

        Trace =    -0.9999993982,   ;   spin precession acos((trace-1)/2) =    179.9555530060 deg
        Precession axis : ( 0.4626,  0.8866, -0.0007) -> angle to (X,Y) plane, angle to X axis :  -0.0426,   -0.0921  degree
        Spin  tune Qs (fractional) :    4.9988E-01
```

As expected for a ring with one snake, n_0 lies in the horizontal plane and the spin tune is 0.5.

Question 14.1.2.5-3 and 4: Figure 14.41 compares the polarization behavior in the AGS Booster lattice with a solenoidal snake for the spin-matched and spin-mismatched snake configurations. From the beam dynamics point of view, the two configurations are similar. They only differ by rotation of the snake section by 90° about the longitudinal axis. However, in the spin-mismatched case, the spin diffusion rate is several times greater than in the spin-matched situation. This result illustrates the effect of proper optics design on the spin dynamics and the importance of spin matching. Note that spin diffusion is present in the matched case as well. It cannot be avoided in this ring configuration due to $\mathbf{n}_0$ being horizontal in the arcs at a sufficiently high synchrotron radiation rate. This scenario is used for demonstration purposes only. It shows that spin diffusion due to improper spin matching can dominate over other depolarizing effects.


Fig. 14.41 Polarization of 100 electrons as a function of the turn number in the AGS Booster lattice with a solenoidal snake for the spin-matched (red) and spin-mismatched (blue) snake configurations
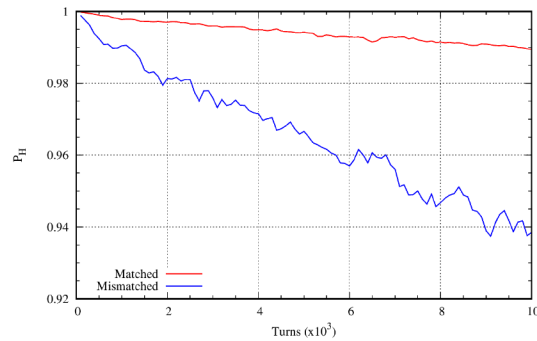
Appendix

A run of Zgoubi code, in addition to zgoubi.res execution listing, and depending on user's requests, may produce various output files. An instance is zgoubi.plt which stores particle coordinates, spin coordinates, electric and magnetic field vectors, etc., step-by-step across optical elements. Another instance is zgoubi.fai which can be used for turn-by-turn particle data storage during multiturn tracking in a circular accelerator. In the present problems, data treatment and graphs can be obtained by reading these files, using gnuplot for instance, or Zgoubi graphic/data treatment interface program Zpop [3]. A brief introduction to these aspects of code and output data handling is given below, and all details can be found in Zgoubi Users' Guide regarding the many storage files at disposal; besides, guidance is provided in due place in the problem assignments (Sec. 14.1) and their solutions (Sec. 14.2).
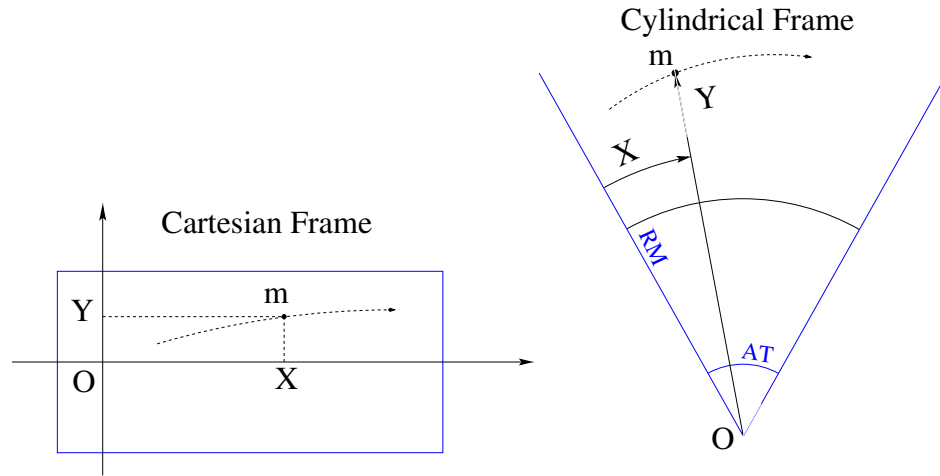
Fig. 14.42 Cartesian and cylindrical reference frames in optical elements. Let a particle location M(X,Y,Z) project to m(X,Y) (the dashed curve shows the projected trajectory). In the case of an optical element defined in Cartesian coordinates (shown here as a rectangular box; for instance, the cases of *BEND*, *MULTIPOL*), X and Y in zgoubi.plt denote the coordinates taken along the reference frame axes. In the case of an optical element (depicted here as an angular sector AT with some reference radius RM) (for instance, the case of *DIPOLE*[*S*]), X is the polar angle, counted positive clockwise, Y is the radius

- Data analysis and plotting:
  - in the matter of graphics it is foreseeable to achieve about any type of graphic, from Zgoubi output files, using gnuplot; if data analysis and other averaging are needed it can be managed via gnuplot scripts (using for instance awk commands, external programs, etc.);

- an additional possibility is to use Zpop, which is part of Zgoubi package. Zpop provides most of the data treatment and graphics means needed to analyze and display the contents of Zgoubi output files.

Besides the run listing zgoubi.res, the main two Zgoubi output files, generally used for data analysis or graphics, are zgoubi.fai (created when introducing the keyword FAISTORE (or FAISCNL, similar), it stores local particle data next to an optical element), and zgoubi.plt (filled up if the flag IL=2 is present in optical elements: it logs step-by-step particle and field data, during numerical integration through the element).

Many additional files can be produced (usually by means of a PRINT argument in a keyword, see the Users Guide), for instance to log data produced by various optical elements and commands, during ray-tracing, in view of data treatment, plotting, debugging, etc. Instances are SPNPRT[PRINT] (spin data logged in zgoubi.SPNPRT.Out), SRLOSS[PRINT] (synchrotron radiation Monte Carlo data logged in zgoubi.SRLOSS.Out).

- Keywords in Zgoubi: by "keyword" it is meant, the name of the optical elements (such as BEND, MULTIPOL, WIENFILT), or input/output procedures (such as FAISCEAU, FAISTORE, SPNPRT, SRPRNT), or commands (such as REBE-LOTE, TWISS, FIT, GOTO, SYSTEM), as they appear in a simulation input data file. Keywords are most of the time referred to without any additional explanation in the exercises: details and explanations regarding the use and functioning of keywords are to be found in the Users' Guide [1].

- It is recommended, when setting up the input data files to work out the simulations, to have Zgoubi Users' Guide at hand. PART B of the guide in particular, details the formatting of the input data which follow most keywords, and their units (a few keywords only, for instance FAISCEAU, MARKER, do not require additional data). PART A is the "physics content" and details what keywords are doing and how. The Users' Guide INDEX is a convenient tool to navigate keywords. A complete list may also be found in the "Glossary of Keywords" Sections, at the beginning of both PART A and PART B, and an overview of what they can be used at is given in "Optical elements versus keywords" Sections.

  – A concise notation KEYWORDS[ARGUMENT1, ARGUMENT2, ...] may be used in the assignments: it follows the nomenclature of the Users' Guide, Part B. A couple of examples:
    · OBJET[KOBJ=1] stands for keyword OBJET, and the value of KOBJ=1 retained here;
    · OPTIONS[CONSTY=ON] stands for keyword OPTIONS, and the option retained here, CONSTY, switched ON.
  – The keyword INCLUDE is used at times. The goal is mostly to modularize input data sequences, with usually the benefit of reduced file lengths and improved clarity. In a very similar way to the Latex or Fortran "include" command, a segment of an optical sequence subject to an INCLUDE by a parent input data file, may always be replaced by that very sequence segment, in the parent file.

- (O;X,Y,Z) coordinates in an optical element: this is the coordinate system in which the field $\mathbf{E}(X, Y, Z)$ and/or $\mathbf{B}(X, Y, Z)$ is defined (the origin for X depends on the optical element). Depending on the optical element concerned, this (O;X,Y,Z) reference frame may be

  - either Cartesian, in which case X, Y, and Z denote the particle position in that frame, T and P the horizontal and vertical trajectory angles (Figs. 1, 2 in the Users Guide, and Fig. 14.42 here),
  - or cylindrical, in which case, given m the projection of particle position M in the Z=0 plane (Fig. 14.42), Y denotes the radial coordinate: $Y = |\mathbf{Om}|$, whereas X denotes the polar angle $\mathbf{OX}$-$\mathbf{Om}$ (as a matter of fact, the nature of the variables named X and Y in the source code does change, and in zgoubi.plt as well) T is the horizontal trajectory angle with respect to the normal to $\mathbf{Om}$, P is the vertical trajectory angle.

References

1. F. Méot: The ray-tracing code Zgoubi, NIM A 767 (2014) 112-125.
   Zgoubi Users' Guide: https://sourceforge.net/p/zgoubi/code/HEAD/tree/trunk/guide/Zgoubi.pdf.
   Zgoubi download package at sourceforge:
   https://sourceforge.net/p/zgoubi/code/HEAD/tree/trunk/
2. gnuplot portable command-line driven graphing utility: http://www.gnuplot.info/
3. Zpop graphic/data treatment interface to zgoubi output files. See Zgoubi Users' Guide [1], PART D, Sec. 1. Zpoo code package is part of Zgoubi download package at sourceforge https://sourceforge.net/p/zgoubi/code/HEAD/tree/trunk/
4. Tygier, S., Kelliher, D: PyZgoubi.
   https://zenodo.org/record/3597426
5. zgoubidoo python interface to zgoubi: https://ulb-metronu.github.io/zgoubidoo/
6. Zgoubi on Sirepo by Radiasoft: https://www.sirepo.com/en/apps/particle-accelerators/
7. Grote, H., Iselin, F. C.: The MAD Program, User's Reference Manual. CERN/SL/90-13 (AP) Rev. 5 (April 29, 1996)
8. USPAS Summer 2021 Spin Class, mini-workshop, helion files repository:
   https://sourceforge.net/p/zgoubi/code/HEAD/tree/trunk/exemples/uspasSpinClass_2021/mini-workshop/AGSBooster_helion/
9. Bai, M.: Overcoming the Intrinsic Spin Resonance in AGS by Using an RF Dipole. PhD thesis, Indiana University, 1999.
   URL https://www.rhichome.bnl.gov/RHIC/Spin/papers/baithesis.pdf.
10. USPAS Summer 2021 Spin Class, mini-workshop, electron files repository:
    https://sourceforge.net/p/zgoubi/code/HEAD/tree/trunk/exemples/uspasSpinClass_2021/mini-workshop/AGSBooster_electronPolarization/
11. https://en.wikipedia.org/wiki/Algorithms_for_calculating_variance#Online_algorithm;
    https://stackoverflow.com/questions/42677017/plot-average-of-nth-rows-in-gnuplot.
    Welford, B.P.: Note on a method for calculating corrected sums of squares and products. Technometrics 4 (3): 419-420. doi:10.2307/1266577. JSTOR 1266577 (1962)